Tectono-stratigraphic development of a salt-influenced rift margin; Halten Terrace, offshore Mid-Norway

Gavin M. Elliott*[1], Christopher A-L. Jackson[1,2], Robert L. Gawthorpe[3], Paul Wilson[2,6], Ian R. Sharp[4] & Lisa Michelsen[5]

[1] Basin Research Group (BRG), Department of Earth Science & Engineering, Imperial College London, London, UK

[2] Department of Earth and Environmental Sciences, University of Manchester, Manchester UK

[3] Department of Earth Sciences, University of Bergen, Norway

[4] Equinor Research Centre, Sandsliveien 90, Bergen, Norway

[5] Equinor ASA, Margrethe Jørgensens vei 4, Harstad, Norway

[6] Now at: Schlumberger Oilfield UK PLC, Schlumberger House, Gatwick, UK

*Corresponding Author Email: gavinmelliott@gmail.com

1. Abstract

Pre-rift salt controls structural style variability within rifts by decoupling sub- and supra-salt faults. However, the way in which this variability controls sediment erosion and dispersal, and facies distributions within the coeval syn-rift stratigraphic succession, remains poorly known. We here use 3D seismic reflection and borehole data to study the tectono-stratigraphic development of the Halten Terrace, offshore Mid-Norway, a salt-influenced rifted margin formed during Middle to Late Jurassic extension. On the eastern basin margin the rift structural style passes southwards from an unbreached extensional growth fold dissected by numerous horst and graben (Bremstein Fault Complex), into a single, through-going normal fault (Vingleia Fault Complex). This southwards change in structural style is likely related to the pinch-out of or a change in the dominant lithology (and thus rheology) within a pre-rift (Triassic) evaporite layer, which was thick and/or mobile enough in the north to decouple basement- and cover-involved faulting, and to permit extensional forced folding. As a result, the salt-influenced Bremstein Fault Complex underwent limited

footwall uplift, with minor erosion of relatively small horsts supplying only limited volumes of sediment to the main downdip depocentre. In contrast, the Vingleia Fault Complex, which was directly coupled to basement, experienced significant uplift and extensive footwall erosion. The footwall of this structure also locally underwent salt-detached gravity gliding and collapse as the pre-rift detachment was tilted. Our results show that where through-going normal faults develop along the rift flanks, the presence of a pre-rift salt layer will suppress the topographic expression of the footwall. The pre-rift salt layer may however facilitate footwall collapse and limit the volume of sediment supplied to downdip basins. Our results also show that variable topography along the rift flanks facilitated the development of relatively small, localised, intra-rift flank accommodation that trapped flank-derived sediment, and which meant basins nearer the rift axis were starved of sediment.

2. Introduction

Several tectono-stratigraphic models have been produced for rift systems developed in predominantly brittle basement (pre-rift) rocks (Prosser 1993; Gawthorpe & Leeder 2000; Ravnås et al., 2000; Withjack et al., 2002). These models predict that rift systems will evolve from an initial stage characterised by numerous, small, isolated normal faults defining relatively subdued topography (rift-initiation), to a stage where extension is focussed on fewer, larger faults systems bounding large half-graben depocentres and prominent topographic highs (rift-climax) (Prosser 1993; Gawthorpe & Leeder 2000; Ravnås et al., 2000). This process of so-called ‘strain localisation’ controls the interplay between the size and location of structurally produced accommodation, sediment source areas, and sediment transport pathways, which together control the syn-rift stratigraphic evolution of a rift system and its constituent basins (Gupta et al., 1998; Gawthorpe & Leeder 2000; Withjack et al., 2002). For example, during the rift initiation low fault slip rates result in only limited accommodation, and because sediment accumulation rates may exceed the rate of accommodation development, basins may be overfilled at this time. In contrast, during the rift climax, fault slip rates, basin subsidence rates, and the rate of accommodation development may be greater than the sediment accumulation rate, resulting in under-filled basins (Gawthorpe et al 1994; Gawthorpe & Leeder 2000). During the rift-climax, footwalls may also become major intra-rift sediment sources, with margin-sourced material being trapped in more proximal depocentres (Underhill et al., 1997; McLeod & Underhill 1999; Welbon et al., 2007; Bilal et al., 2018).

In rifts containing salt within the pre-rift stratigraphy, these existing tectono-stratigraphic rift models may not be applicable because salt flow may modify or fully overprint the uplift and subsidence patterns related to normal faulting and associated folding (Withjack et al., 1990; Richardson et al., 2005; Marsh et al., 2010; Duffy et al., 2012; Rowan 2014; Jackson & Lewis 2016; Tavani & Granado 2015; Tavani et al., 2018; Jackson et al., 2019). Pre-rift salt may also act as an intra-stratal detachment, partially or fully decoupling the sub-salt basement-involved and supra-salt cover-restricted structures accommodating extension (Withjack et al., 1990; Richardson et al., 2005; Marsh et al., 2010; Rowan 2014; Coleman et al., 2019). Fault-propagation folding, which is related to the vertical propagation of structures through the evaporite, may also be more common in salt-influenced rifts (Withjack el al 1990; Corfield & Sharp 2000; Coleman et al., 2019). The geomorphology and tectono-stratigraphic evolution of salt-influenced rifts may therefore differ to that of salt-free rifts (Gawthorpe & Leeder, 2000; Withjack et al., 2002). Existing rift basin models also lack a temporal framework within which to understand timing of erosion and sediment supply within the evolving rift system.

In this paper we couple structural and seismic-stratigraphic mapping from 3D seismic reflection and borehole data along the Halten Terrace, offshore Mid-Norway to determine the role that relatively thin (<500 m), pre-rift salt had on the late Middle Jurassic to Early Cretaceous (~27 Myr) syn-rift tectono-stratigraphic development of a rifted margin. Thanks largely to the moderate burial depths of the rift, which permits good quality seismic imaging of the stratigraphic section from Paleozoic to recent, in addition to the relatively large number of wells with biostratigraphic data, we can establish the rift structure and erect a basin-wide, age-constrained, syn-rift stratigraphic framework within which to understand the timing of erosion and sediment supply. Integration of sub-crop mapping along the footwall of the major border faults, combined with seismic stratigraphy of the hangingwall depocentres, also allowed us to demonstrate the impact the pre-rift salt had on the structural configuration of the rift flanks which in turn determined the volume and flux of sediment delivered to adjacent depocentres.

3. Geological setting

3.1 Structural framework of the Halten Terrace

The Halten Terrace is an 80 km wide by 130 km long, normal fault-bounded structural terrace that is located between 64° and 65° 30’N on the Mid-Norwegian continental shelf (Figure 1) (Blystad et al., 1995; Zastrozhnov et al., 2020). The area has been subject to a complex, long-lived, multi-phase extensional history, from post-Caledonide (i.e., Devonian) extensional collapse and Permo-Triassic and Late Jurassic rifting, through to the opening of the NE Atlantic in the Cenozoic. The Late Jurassic-Early Cretaceous extensional phase forms the focus of this paper (e.g. Bukovics et al., 1984; Blystad et al., 1995; Doré et al., 1997; 1999; Roberts et al., 1999; Brekke, 2000; Faleide et al., 2008; Peron-Pinvidic & Osmundsen 2018; Bunkholt et al., 2021).

The structural evolution of the Halten Terrace results, in part, from the interaction between late Middle Jurassic-Early Cretaceous rift-related normal faults and a thin (< 500 m) pre-rift, Triassic, evaporite-dominated unit (Jacobsen and van Veen, 1984; Wilson et al., 2015). This unit served to variably decouple rift-related deformation in sub- and supra-salt strata, resulting in the development of extensional fault propagation folds, and basement-involved and basement-detached normal faults (Figure 1c) (Withjack et al., 1989; Pascoe et al., 1999; Corfield and Sharp, 2000; Dooley et al., 2003; Richardson et al., 2005; Marsh et al., 2010; Wilson et al., 2013; 2015; Tavani & Granado 2015; Tavani et al., 2018). In contrast to other salt-influenced rift basins such as those found in the Southern Northern Sea (Stewart et al., 1997; Richardson et al., 2005; Kane et al., 2010; Rowan 2014; Jackson et al., 2019) the Halten Terrace salt, despite being relatively thin and non-diapiric, exerts a strong influence on the tectono-stratigraphic evolution of the basin.

We focus on the southern and eastern margins of the Halten Terrace. Here, the N-S trending Bremstein and NE-SW trending Vingleia fault complexes separate the Trøndelag Platform and Frøya High from the Gimsan Basin (Figure 1) (Wilson et al., 2015). The Vingleia Fault Complex merges to the south with the N-S-striking, Klakk Fault Complex and the Sklinna Ridge, which together define the western limit of the Halten Terrace (Figure 1 & 2) (Blystad et al., 1995). Internally, the Halten Terrace contains numerous Triassic-to-Jurassic, tilted normal fault blocks and sub-basins, with the elliptical, 2200 km^2, N-S trending Gimsan Basin representing one of the largest syn-rift depocentres on the Halten Terrace (Figure 1 & 2) (Blystad et al., 1995). Internally the Gimsan Basin comprises of two sub-basins, informally referred to here as the North and South Gimsan basins; these sub-basins are separated by a basement-involved structure that is expressed as a monocline at Upper Jurassic levels (Figure 2).

The Bremstein Fault Complex (BFC) is a supra-salt, cover-restricted fault system that detaches downwards into the Triassic salt where the top (but not base) salt level is clearly offset (Wilson et al., 2013; 2015). The pre-rift cover is offset only a modest amount across the BFC and is instead defined by a major fault-related monocline that is cut by numerous faults with small throws (Figure 2). Wilson et al. (2013) show that the degree of linkage between sub- and supra-salt restricted structures were controlled by vertical strain partitioning across the Triassic salt. This meant that sub-salt and supra-salt fault populations acted as kinematically semi-independent systems, i.e., some of the supra-salt faults were partly gravity-driven and related to tilting of the salt in response to basement-involved faulting, whereas others directly accommodated thick-skinned (i.e., sub-, salt-, and supra-salt involved) extension. In contrast, the Vingleia Fault Complex (VFC) offsets the salt and pre-rift package, with basement-involved, NE-SW-striking, large-throw faults that dip to the NW defining the northwestern flank of the Frøya High (Figure 1). The footwall of the VFC is characterised by a narrow zone of relatively low throw faults that either detach into or near to the top of salt layer (Wilson et al., 2015). The Frøya High is a N-S trending, normal fault-bound, granite-cored horst that is ~ 120 km long and up to 40 km wide (Blystad et al., 1995; Slagstad et al., 2011). The along-strike variation in structural style, from a zone of diffuse faulting and an unbreached fault-propagation fold (i.e. the Bremstein Fault Complex) to a narrow zone of focused deformation (Vingleia Fault Complex), is key to the syn-rift tectono-stratigraphic evolution of the eastern margin of the Halten Terrace and is the focus of this study.

At the regional scale, the NE-trending fault trends that define the Vingleia, Ytreholmen and Revfallet fault complexes are thought to be inherited from the earlier Late Permian-Early Triassic rift episode (Figure 1). Similar fault trends are evident in the Froan Basin and Trøndelag Platform, and are associated with thick Permo-Triassic (syn-rift) growth wedges (Bunkholt et al., 2021). This fault trend on Halten Terrace may therefore indicate that the NE-trending Vingleia fault trend is both inherited and long lived.

3.2 Stratigraphic framework of the Halten Terrace

The Early Jurassic to early Middle Jurassic stratigraphy comprises paralic-to-shallow-marine, sandstone- (Garn,Ile & Tofte formations) and mudstone-rich (Not & Ror formations) units that record deposition during the late pre-rift to early syn-rift period (rift initiation; Figure 3) (Gjelberg et al., 1987; Dalland et al., 1988; Swiecicki et al., 1998; Martinius et al., 2001; 2005; Messina et al., 2014). The late syn-rift period occurred during the late Middle Jurassic to Early Cretaceous, and was characterised by accelerated rates of extension and normal fault-controlled subsidence. Increasing rates of accommodation generation resulted in drowning of the Halten Terrace and deposition of an open marine, mudstone-dominated succession (Melke and Spekk formations) (rift climax; Figure 2) (Dalland et al., 1988; Swiecicki et al., 1998). However, some of the largest basement-cored structural highs were sub-aerially exposed during the Late Jurassic and were flanked by relatively coarse-grained, clastic depositional systems (e.g. Intra-Melke sandstones and Rogn Formation) (Dalland et al., 1988; van der Zwan, 1990; Provan, 1992; Chiarella et al., 2020; Jones et al., 2021). The Rogn Formation, which is composed of highly bioturbated, fine-to-medium grained sandstones in the Draugen Field, is located on the footwall of the Vingleia Fault Complex (Figure 1). Traditionally, the Rogn Formation has been interpreted as a ‘detached’, shallow marine bar system, deposited tens of kilometres from the contemporaneous shoreline (van der Zwan, 1990; Provan, 1992). However, Chiarella et al. (2020) propose that the Rogn Formation represents a tidally influenced sand body deposited on a shallow shelf.

Coarse clastic units broadly age-equivalent to the Melke and Rogn Formation (Oxfordian to Kimmeridgian/Tithonian) are drilled in the hangingwall of the Vingleia Fault Complex where it defines the edge of the basement-cored Frøya High (Elliott et al., 2017; Jones et al 2021) (Figure 1). Here, the Fenja Discovery is hosted in Middle to Late Oxfordian (Melke Formation) and Kimmeridgian (Spekk Formation), coarse clastic hangingwall fans (Jones et al 2021). The nearby Bue discovery is hosted within Kimmeridgian to Tithonian Rogn Formation clastics (Jones et al 2021). Despite new data being provided by these relatively recent boreholes, the lithology, facies, and tectono-stratigraphic context of the Melke and Spekk formations are poorly documented across the wider Halten Terrace; this forms the focus of the current study.

4. Dataset and Methodology

Stratigraphic and structural mapping was mainly conducted on four time-migrated, 3D seismic reflection datasets that cover ~ 3200 km^2 of the southern Halten Terrace (Figure 1). These 3D volumes were tied to 2D seismic reflection profiles to provide a basin-scale context to the detailed stratigraphic and structural observations and interpretations (Figure 1). The 3D seismic volumes have an inline and crossline spacing of 12.5 m. The vertical (depth) axis is measured in milliseconds two-way time (ms TWT) and the seismic data have a vertical record length of 5500 ms TWT. Frequency analysis of these seismic data, when combined with an understanding of the interval velocity within the stratigraphic interval of interest, indicates that the vertical resolution within the interval of interest is 20 - 30 m (Figure 3). The seismic data were tied to exploration wells using synthetic seismograms, allowing stratigraphic ages (using the framework of Dalland et al., 1988) to be assigned to mappable seismic reflections and permitting a direct lithological calibration of the syn-rift seismic facies (Figure 3). Although the seismic reflection events can be mapped over the basin to define the main seismic-stratigraphic packages, intra-package lateral facies changes mean that the lithostratigraphic terminology *within* seismically defined units varies spatially (Figure 3). Isochron (thickness) maps were generated to investigate spatial variations in stratigraphic thickness away from areas of well control; thickness variations were used to identify syn-depositional structures and depositional elements. We also mapped subcrop patterns below and onlap patterns above, the major unconformities in the footwall of the Vingleia Fault Complex to examine the timing and depth of erosion, and the potential provenance of sediments contained within the adjacent depocentres.

We used 17 key wells containing a full suite of petrophysical well logs (Table 1 & Figure 1b). Twelve of the wells are located along the footwalls of the Bremstein and Vingleia fault complexes, with the remainder in the Gimsan Basin to the west (Figure 1b). Very little Upper Jurassic core has been cut in the study area, thus the lithology and facies of units has been inferred from well cuttings reports, linked to petrophysical well-log characteristics and the overall tectono-stratigraphic context of individual wells and units (e.g. structural and stratigraphic position within the syn-rift succession). Thirteen of the wells had proprietary biostratigraphic data that allowed the ages of key stratal surfaces to be constrained and facilitated the construction of chronostratigraphic correlation panels. Seismic profiles that passed between wells were used to provide a tectono-sedimentary context to the stratigraphic data (e.g. stratal thickening across syn-depositional normal faults) in these panels and to quality control the correlation itself.

5. Rift flank

5.1 Rift flank structural configuration

The BFC is characterised by westward-dipping strata that define a 15 km wide monocline limb dissected by numerous supra-salt normal faults that tip out into or onto the salt layer (Figure 4a) (Withjack et al.,1989; 1990; Dooley et al., 2003, Wilson et al., 2013; 2015). The supra-salt faults strike N-S, are up to 20 km long, and have up to 650 ms TWT throw, and are both antithetic (i.e., east-dipping) and synthetic (i.e., west-dipping) to the sub-salt master fault (Figures 4a). The BFC varies geometrically along its length; in the north of the study area, it is bound to the west by a basement-involved normal fault that has a listric normal fault in its footwall at Upper Jurassic levels (Figure 1c). Further south, the BFC is characterised at Upper Jurassic levels by a fault-parallel, faulted monocline developed above major sub-salt faults (Figure 4a). Wilson et al. (2013) show that localised throw minima on these faults likely represent the position of breached relay ramps that developed as individual fault segments grew and linked.

The transition from the BFC to VFC is defined by a southward change in strike from N-S to NE-SW at all stratigraphic levels. This change in strike is most likely due to the Jurassic to Earliest Cretaceous rift faults locally reactivating intra-basement structures inherited from possible Caledonian or Permo-Triassic origin (Wilson et al., 2015). A distinct change in structural style occurs southwards, with a major faulted monocline overlying a single basement-involved normal fault (BFC) passing into a fault complex characterised by distributed, basement involved faults (VFC) (Wilson et al., 2015). Wilson et al. (2015) use seismic facies analysis (due to the lack of well control in the evaporite layer in the study area) to suggest that the change in structural style could also be related to facies changes within the evaporite sequence, i.e., ductile, halite-dominated units that decoupled sub- and supra-salt strain and permitted forced folding, pass southwards into more brittle, halite-poor units that permitted through-going (i.e., across-salt) faulting.

The VFC is characterised by basement-involved normal fault systems that offset the pre-rift and Triassic salt packages by up to 2 sec. TWT (Figure 4b). The hangingwall of the VFC is defined by a 30 km long and 5-10 km wide, fault-parallel syncline, whereas the footwall is characterised by several gently rotated fault blocks (Figure 4b). The footwall fault blocks are up to 2 km wide, bounded by broadly NE-SW striking normal faults that have up to 150 ms TWT of throw and are up to 5 km long (Figure 4). These faults are downthrown to progressively deeper structural levels towards the NW (i.e. into the hangingwall), and in cross-section they detach downwards into the Triassic salt layer, which dips and deepens westwards (Figure 4b). The majority of the faults downthrow to the NW, but a distinct NE-SW striking horst block (labelled A in Figure 4b), bounded on its south-eastern side by a SE-dipping normal fault, defines the eastern limit of tilting and faulting in the footwall of the VFC. East of this horst the footwall is relatively undeformed, forming a gently eastward-dipping structural terrace (Figure 4b).

5.2 Rift flank erosion

The Triassic and Jurassic stratigraphy along the westernmost edge of the Trøndelag Platform are of relatively uniform thickness (~ 1300 ms TWT thick), although the BCU progressively erodes into deeper stratigraphic levels such that Lower Cretaceous strata directly overlie Lower Jurassic strata in the south (Figure 5). In the footwall of the BFC the Jurassic section thins westwards towards the fault complex over a lateral distance of 10 km. This thinning is related to the gradual downcutting of the BCU towards the fault complex, with localised deeper erosion found in the immediate footwall of the easternmost fault in the Bremstein Fault Complex (see also Elliott et al., 2012).

The equivalent succession in the footwall of the VFC strongly contrast with that observed in the north next to the BFC, i.e., it is more variable in thickness (1200 – 0 ms TWT), ultimately thinning towards the footwall crest of the fault complex, where it is locally absent or below seismic resolution. The boundary between these two styles of erosion is co-incident with a NE-SW-striking basement-involved normal fault that breaches the salt and BCU, and that tips out within the lowermost Cretaceous interval (Figure 5). It is possible that this fault could represent the NE continuation of the VFC onto the Trøndelag Platform.

5.2.1 Bremstein Fault Complex

The style of erosion in the footwall of the BFC varies along strike. First, there is a region of localised footwall erosion that extends up to 3 km into the footwall of the easternmost fault within the complex (Figure 6a). Erosion here defines drainage catchments that are up to 7 km^2 in area and which display erosional relief of up to 150 m (Figure 6a) (see detailed description by Elliott et al. 2012).

In contrast to the relatively organised style of erosion described by Elliott et al., (2012), which is only locally developed, the majority of fault blocks that comprise the BFC have undergone gravitational collapse. In one example, footwall collapse has occurred along listric faults that detach into the mudstone-dominated Ror Formation (Figure 7). A consequence of the footwall collapse is that crests of individual blocks within the fault complex are characterised by arcuate scarps that have resulted from the downslope translation and rotation of blocks that are up to 1.5 km wide and 750 m long (Figure 7).

The complex and varied topography that developed along the length of the BFC during the Middle to Late Jurassic provided localised depocentres within the normal fault complex itself (Figure 8). The sediment contained within these depocentres is likely to have been locally sourced from the crests of intra-complex fault blocks.

Two key observations suggest erosion of these fault blocks and related syn-rift deposition occurred in the Oxfordian. First, well 6407/6-7S, which is located in the hangingwall of the easternmost fault and downdip of the erosional catchments, cored an 18 m thick, Oxfordian turbidite-bearing succession with an otherwise mudstone-prone succession (Melke Formation) (Figure 8a). Second, well 6407/6-4, which is located within the BFC, penetrated a 100 m thick, fine-grained siltstone-dominated, syn-rift succession (Melke Formation) in unconformable contact with the underlying Garn Formation across a Middle Oxfordian erosional surface (Figure 8b).

5.2.2 Vingleia Fault Complex

Seismic data indicate that erosion level along the footwall of the VFC is deepest in the immediate footwall and increases southwards towards the Frøya High (Figure 5). In contrast to the BFC, the footwall of the VFC is characterised by a gently eastward-dipping, peneplain-like surface and a series of westward-dipping, erosionally capped fault-bound terraces (Figure 9).

Seismic mapping in the footwall of the VFC reveals that the Upper Jurassic succession is relatively thin (typically <100 ms TWT; Figure 9), meaning the erosional history and style in this location cannot be resolved by using seismic data alone. However, by using biostratigraphically-constrained well correlation panels, we can assess the variability in erosion levels in the VFC footwall. These stratigraphic data reveal that three major erosional unconformities are developed in the Middle to Upper Jurassic syn-rift succession in this location (Figure 9 & 10). The lowermost unconformity, which is Early Callovian and that defines the top of the Garn Formation, is mapped across the entire footwall (including to the E of the NE-SW-striking horst) suggesting it was not simply formed due to relatively local, fault-driven uplift. The Early Callovian unconformity dips gently to the east and is progressively onlapped by Middle to Late Callovian strata (Melke Formation; Figures 9 and 10).

A younger, early Oxfordian unconformity is developed above and locally merges with the early Callovian unconformity on the flanks of the NE-SW-striking horst (labelled A in Figure 9), where it forms part of a composite, erosional unconformity capping the VFC (Figure 9 & 10). An important observation is that the composite unconformity can be traced within the rotated fault blocks at different structural elevations; combined with the fact that the units above and below the unconformity in 6407/8-4S are of similar age to that observed in 6407/9-4, these observations suggest that the footwall was a single structure when the unconformity formed during the early Oxfordian, and that it was subsequently dissected by normal faults (Figure 9). The prominent NE-trending horst (A in Figure 9) has been relatively deeply eroded, removing the Melke and Garn formations, resulting in the Spekk Formation (Tithonian) sitting directly on the Not Formation (Bajocian) in well 6407/9-9 (Figure 9). East of the horst, Kimmeridgian-to-Early Tithonian shallow marine shoreface sandstone of the Rogn Formation were deposited directly on the Early Oxfordian unconformity (Figures 9 & 10). The Late Tithonian-to-Berriasian Spekk Formation can be traced across the footwall of the VFC, where it is overlain by Early

Cretaceous strata across the Base Cretaceous Unconformity, the third and final unconformity identified along Vingleia Fault Complex (Figures 9 and 10).

6. Hangingwall Depocentre: the Gimsan Basin

The Gimsan Basin defines the hangingwall of the Bremstein and Vingleia fault complexes (Figures 2 & 4). The basin comprises several sub-basins, with the two main depocentres separated by a NE-trending structural high that overlies the footwall of an underlying, basement-restricted, blind normal fault that splays off from the BFC (Figures 5 & 11).

The Middle to Late Jurassic succession in the Gimsan Basin is characterised by moderate- to low-amplitude, semi-continuous reflections. We map two main seismic units within the Gimsan Basin that correspond to the Melke and Spekk formations based on well ties (Figure 11). The base of the Melke Formation is represented by a prominent reflection event and although the absolute age of this horizon is poorly constrained, regional chronostratigraphy data suggest it is Bathonian (Dalland et al., 1988) (Figure 3). The Melke Formation is up to 400 ms TWT thick in the largest sub-basin, which is located in the SE in the immediate hangingwall of the VFC, and up to 150 ms TWT in the smaller, north-western depocentre (Figure 11). Five wells have at least partly penetrated the Melke Formation; three of these are located around the margins of Gimsan Basin and two are located close to the intra-basin high (Figure 12). Cuttings and well-log data suggest the formation is dominated by claystone and thin, very-fine to fine-grained sandstone and carbonates in the deepest part of the basin (e.g. 6407/8-1 and 6407/5-1; Figure 12). Towards the basin flanks the formation thins; here, interbedded siltstones and carbonates are the dominant lithologies (e.g. 6407/2-1, 6407/7-8 & 6407/4-1; Figure 12). In the immediate hangingwall of the VFC the Melke Formation is characterised by several relatively high-amplitude, mounded, convex-up packages of seismic reflections that downlap the Top Garn reflection (Figure 13). These mounded bodies are up to 200 ms TWT thick, extend up to 4 km away from fault, and can be traced for 10 km parallel to the fault (Figure 13). In detail, individual mounded bodies exhibit a compensational stacking pattern, with stratigraphically younger mounds onlapping underlying mounds and with their axes offset from the crests of the older mounds (Figure 13b). Although assigned to the Melke Formation, these submarine fans could range in age from Bathonian to Oxfordian (Figure 3), and in the absence of well data their age remains unknown. We propose they are Oxfordian based observations to the south of the study area, where Intra-Melke sandstone and conglomeratic bodies, are also situated in the hangingwall of the VFC, but which were deposited in a different sub-basin, form the lower reservoir in the Fenja discovery (Jones et al., 2021). These clastics are dated to be Middle to Late Oxfordian, and are interpreted to be hangingwall fan deltas deposited above a mudstone-dominated, Callovian-Bathonian to Early Oxfordian, Lower Melke Formation (Jones et al., 2021).

The boundary between the Melke Formation and the overlying Spekk Formation is defined by a change to higher-amplitude reflections that well data indicate corresponds to a change to a more claystone-dominated lithology (GR values >150 API) with rare, thin sandstones and carbonates (Figure 12). The Spekk Formation is up to 700 ms TWT thick and is thickest in the south, in the immediate hangingwall of the VFC (Figure 11). Seismically, the Spekk Formation is characterised by low-amplitude, semi-discontinuous reflection events; distinct seismic geomorphological features, such as the mounded features in the underlying Melke Formation, are not observed (Figure 14a). More coherent, moderate-amplitude reflections are locally developed, with an reflection mean strength (RMS) amplitude extraction around one such event revealing several curvilinear, convex-to-the-west, high-amplitude lineations striking parallel to the BFC (Figure 14b). Similar features are imaged by Løseth et al. (2011) in the overlying Lange Formation (Lower Cretaceous) and in well 6407/5-1, where a section of deformed Late Jurassic Spekk Formation is encased in the younger, Early Cretaceous Lange Formation. We interprete these arcuate features as the seismic expression of a 50 m thick Spekk Formation slide complex, sourced from the BFC and that translated westwards into the Gimsan Basin. A RMS extraction taken from our dataset through the Lower Cretaceous slide complex described by Løseth et al. (2011) reveals a series of curvilinear lineations similar to those we have mapped and imaged in the Spekk Formation. Thus, by analogy, we interpret the curvilinear seismic facies in the Spekk Formation to represent a submarine slide complex (Figure 14c). Geometrically comparable features of equivalent age and likely similar oroigin are also evident within the Draupne Formation in the in Tampen Spur area of the Northern North Sea (Løseth et al. 2011).

7. Tectono-stratigraphic development of the Eastern Halten Terrace

The tectono-stratigraphic evolution of the eastern Halten Terrace records the long-term (~ 27 Myr) development of a salt-influenced rift basin. Our chronostratigraphic framework based upon well biostratigraphy allows us to define key tectono-stratigraphic phases. We here outline these phases, which are characterised by distinct, structurally controlled sediment dispersal patterns, at the stage level.

7.1. Rift Initiation

7.1.1. Bathonian (167 – 164 Ma)

Well and seismic data indicate that during the Bathonian, the study area was split into two different depositional regimes. The Gimsan Basin and the footwall of the BFC were represented by shelfal conditions (i.e., Melke Formation) (Figure 15a). The footwall of the VFC was in contrast characterised throughout by shallow marine conditions as recorded in the Garn Formation (Gjelberg et al., 1987; Messina et al., 2014). Well data in the vicinity of Njord and Fenja fields, in the future, deep-water hangingwall of the VFC, also record relatively shallow-marine, shelfal conditions at this time (i.e., Melke Formation) (Jones et al., 2021).

The water depth increase recorded by the vertical change from the Garn to Melke Formation is regionally diachronous across the Halten Terrace, and is associated with an overall transgressive/backstepping motif (i.e., shallow marine sandstones pass upwards into finfer-grained, shelfal heterolithics; Corfield & Sharp 2000, Corfield et al., 2001). There is very little evidence of activity along the BFC during this time, and a gentle monoclinal structure was likely present and associated with subtle bathymetric variations. Accumulation of the Melke Formation siltstones suggest that the footwall of the BFC was submarine during the Bathonian, indicating an overall deepening of the basin northwards from the shallow marine footwall of the VFC (Figure 15a).

Eastwards onlap of the Melke Formation onto the Garn Formation in the Gimsan Basin indicate that, during the Bathonian, the fault systems along the rifts eastern flank were active, but were expressed as an at-surface monocline above a blind normal fault (Figure 11) (i.e. extensional forced fold; Coleman et al., 2019).

7.1.2. Callovian (164 – 161 Ma)

The footwall of BFC was submarine throughout the Callovian, with siltstone (Melke Formation) accumulating in both its footwall and hangingwall (Figure 15b). The VFC continued to grow via tip propagation, resulting in breaching of the basin-margin monocline and the formation of a surface-breaching normal fault that drove uplift its footwall and the formation of a hangingwall half-graben (Figure 15b). Uplift caused sub-aerial exposure and erosion of the immediate crest of the footwall of VFC, which at this time likely represented an intra-rift island (Yielding 1990; Roberts & Yielding 1991; Bell et al., 2014; Roberts et al., 2019). Some of the sediment derived from erosion of the VFC footwall will have been transported eastwards onto the hangingwall dipslope, likely deposited in shallow marine-to-shelfal environments fringing an intra-rift island (Figure 15b).

The lack of coarse-grained clastic deposits on the hangingwall dipslope implies that the Garn Formation was not exposed at the footwall crest at this time and that only relatively fine-grained, Bathonian deposits of the Melke Formation were exposed and reworked (Figure 9 & 10). We infer that the remaining sediment eroded from the intra-rift island was transported westwards into the immediate hangingwall of the Gimsan Basin, which at this time represented a major, deep-marine depocentre (Figure 5b). Accumulation of a relatively fine-grained succession in the Gimsan Basin suggests that the sand-rich Garn Formation was not exposed on the intra-rift island.

7.2. Rift Climax

7.2.1. Oxfordian (161 – 155 Ma)

The presence of Oxfordian turbidites “ponded” within fault blocks of the Bremstein Fault Complex suggest this fault complex was active during the Middle Oxfordian. These turbidites could have been derived from the drainage catchments imaged along the eastern edge of BFC (Figure 6) (see Elliott et al., 2012 for details). A Middle Oxfordian erosional unconformity, recognised in wells next to the Bremstein (e.g. 6407/6-4; Figure 8) and Vingleia fault complexes, indicates a break in sedimentation along the latter and erosion along the former (Figure 15c).

We speculate that during the Oxfordian, the VFC formed a single, through-going normal fault, but that activity on the smaller faults associated with eventual collapse of its footwall may have produced some subtle relief. Erosion of this relief may have the yielded thin sandstones, such as those found within the middle to late Oxfordian of well 6407/6-7S (Figures 8 & 15c). We propose that the mounded seismic facies imaged in the immediate hangingwall of the VFC (Figure 13) are submarine fans derived from erosion from the footwall of the fault complex. Similar gravity-flow emplaced deposits are found in similar hangingwall settings immediately downdip of a degraded fault scarps in the Statfjord East field area, Northern North Sea (Welbon et al., 2007) and in the immediate hangingwall of the VFC to the south of the study area; in the latter case, thick, Oxfordian fan systems are proven (Jones et al., 2021). The majority of the sediment delivered eastwards to the hangingwall dipslope, will have been sourced from the erosion of the underlying Callovian and older shelfal siltstones, resulting in deposition of a relatively fine-grained Oxfordian succession (Melke Formation) (Figures 9 & 10).

The Gimsan Basin continued to accumulate predominantly siltstone (Melke Formation) throughout the Oxfordian, suggesting that the majority of sediment was transported eastwards from the VFC, implying that the regional tilt of the footwall controlled sediment pathways at that time. Along the BFC, the faulted monocline configuration produced numerous localised depocentres that trapped the locally derived sediment, stopping it being delivered westwards to the Gimsan Basin (Figure 15c).

7.2.2. Kimmeridgian to Early Tithonian (155 – 147 Ma)

The BFC is interpreted to have been in a submarine environment during the Kimmeridgian and Tithonian. A transition from the deposition of siltstone-dominated, shelfal sediments during the Kimmeridgian, to claystone-dominated, deep-water deposits during the Early Tithonian, signifies a relative increase in water depth, which may have been of regional extent (i.e., eustatic).

The Kimmeridgian to Early Tithonian represented a period of major clastic input onto the hangingwall dipslope of the VFC and associated deposition of a medium to coarse-grained, shallow marine succession of the Rogn Formation on the eastern flank of the Frøya High (Figure 15d). This time interval represents a phase of salt-detached, gravity-driven extension, faulting, and uplift along the NW-dipping footwall (Figure 15d). This renewed fault activity may have uplifted a section of previously buried Garn Formation, rejuvenating it as a sediment source area. An alternative interpretation is that footwall uplift segmented the basin, with this structurally controlled bathymetry enhancing tidal currents that transported sediment northwards, along strike from the Frøya High.

Footwall collapse may have led to exposure of the evaporite detachment at the seabed, promoting north-westwards (i.e., towards-the-hangingwall) gliding, and stretching and faulting of its overburden (Figure 15d) (*cf*. 'rift-raft tectonics' of Penge et al., 1993). During the Kimmeridgian, the area to the south of Frøya High, the VFC, underwent large-scale collapse, with fault scarp degradation complexes developed in the vicinity of the Fenja Discovery wells (Jones et al., 2021). Similar footwall collapse via block sliding is reported in the Statfjord Field complex when the mudstone-prone Dunlin Group, which was main intra-stratal detachment, was exposed at the seabed (Hesthammer & Fossen 1999; Welbon et al., 2007).

A progressive increase in erosion levels southward along the VFC footwall towards the Frøya High correspond to increased sediment accumulation in the SW corner of the Gimsan Basin (Figure 11b). It is unlikely that the VFC footwall supplied all of this sediment due to its limited size; it is more likely that sediment was channelled from the Frøya High into the Gimsan Basin (via the Njord relay ramp *c.f.* Elliott et al., 2017), greatly enhancing sediment accumulation along with background hemipelagic and pelagic input (Figure 15d). The Gimsan Basin continued to subside relative to the rift flanks, with well data indicating deposition of a claystone-dominated succession (Spekk Formation) and a near-absence of relatively coarse-grained sediment (Figure 12).

7.2.3. Late Tithonian to Berriasian (147 – 140 Ma)

During the Late Tithonian to Berriasian, regional extension continued but was focussed on the Klakk Fault Complex (i.e. west of the Sklinna Ridge; Figure 1). The Bremstein and Vingleia fault complexes were largely inactive as strain migrated westwards. The remnant rift bathymetry was passively infilled and onlapped by deep marine claystone (Spekk Formation) (Figure 15e). The distinctive onlap and flooding surface is represented by the Base Cretaceous Unconformity on both seismic sections and wells. The rift-bounding faults, although not tectonically active, were still associated with significant topography, with mud-prone submarine landslides occasionally occurring along the flanks of individual fault blocks (Figure 15e).

8. The role of salt in controlling the tectono-stratigraphic architecture and evolution of rifts

The presence of the pre-rift salt unit had a profound effect on the tectono-stratigraphic development of not only the Bremstein and Vingleia fault complexes, but also that of the flanking depocentre, the Gimsan Basin. The evaporite layer acted as a temporary (i.e. Vingleia Fault Complex) or permanent (i.e. Bremstein Fault Complex) barrier to the upward propagation of basement-involved faults. The

Triassic evaporites facilitated the development of: (i) fault-related at-surface monoclines; (ii) gravity-driven, supra-salt extensional rafts on the steep, basinward-dipping limb of the fault-related monoclines; and iii) the development of a broad, synclinal growth fold within the hangingwall depocentre (Gimsan Basin) (Figure 16). In the following sections we explore the impact the pre-rift salt unit had on lateral variations in rift flank geometry and how it controlled the location, shape and size of sediment source areas and transport pathways, and thus facies variations within the syn-rift stratigraphic succession.

8.1. Sedimentary Sources and Pathways

The complex depositional topography associated with faulting of the extensional forced fold, and the subsequent rotation of the entire BFC, produced localised intra-rift flank depocentres in the immediate hangingwall of the faults (Figures 4 & 6). This terrace-like fault block topography comprised short, en-echelon fault segments bounding small depocentres that limited sediment delivery to the Gimsan Basin from the Bathonian to the Tithonian (i.e. c. 23 Myr) (Figure 16). In addition, the lack of footwall uplift and prolonged sub-aerial exposure along the footwall limited the area of erosion and the volume of sediment supplied into the Gimsan Basin (Elliott et al., 2012). However, erosion of the relatively small fault blocks did locally occur; where this erosion reworked the sand-rich Garn Formation, Oxfordian turbidites where deposited in small depocentres within the fault complex (Figure 16).

In contrast to the BFC, activity on the salt-breaching VFC drove uplift and erosion of its footwall crest, allowing the release of significantly larger volumes of sediment into the adjacent depocentres (Bell et al., 2014). Although the uplift, rotation, and sub-aerial exposure had the potential to release larger volumes of sediment, large-scale footwall collapse above the salt layer reduced the overall topographic elevation along the crest of the VFC (Figures 4 & 9). In common with the BFC, the development of this raft-related topography led to the deposition of perched sediment accumulations along the footwall of the VFC, comprised largely of older, reworked Jurassic strata.

The deepest erosion levels along the eastern flank of the Halten Terrace are in the south, where the VFC forms the boundary with the Frøya High (Figures 2 & 5). In this area, the areal extent of the evaporite succession is not fully understood due to a lack of well control to calibrate seismic interpretation. However, Wilson et al. (2015) speculate that during evaporite deposition in the Triassic, the Frøya High most likely delimited the edge of the evaporite basin. In such a setting it is common for the less mobile evaporite and evaporite-related sediments, such as anhydrites and carbonates, to be deposited (*c.f.* Permian Zechstein Supergroup of the North Sea, Clark et al., 1998; Jackson et al., 2019). The presence of largely immobile rocks on the flanks of the Frøya High would have inhibited supra-salt footwall collapse, thereby enhancing uplift and associated erosion of the footwall (Figure 5 & 10). The lack of complex footwall topography, which would produce local accommodation along the fault complex, would have allowed direct sediment delivery to the Gimsan Basin; this may explain the greater sediment thicknesses found in the SE corner of the basin (Figure 11). This observation is supported by the recent work of Jones et al. (2021) to the south of the study area.

8.2. Salt-influenced Rift Basin Geometry and Syn-Rift Stratigraphy Style

Low sediment supply from the rift flanks combined with a large amount of structurally controlled accommodation, meant that the Gimsan Basin was largely sediment underfilled (Figure 16). Rift flanks typically supply sediment to the hangingwall basin with this sediment derived from uplift-driven erosion of the immediate footwall (i.e., consequent drainage systems) or longer-lived systems that pre-date rifting (i.e., antecedent drainage systems) (Prosser 1993; Gawthorpe & Leeder 2000; Ravnås et al., 2000). The presence of the pre-rift salt unit has a profound impact on the rift basin geometry as it decouples the deformation above and below the salt unit, determining the degree of salt tectonics in the supra-salt cover that ultimately controlled the syn-rift stratigraphic evolution. By reducing the footwall elevation along the rift flank (*c.f.* Bremstein Fault Complex) sediment supply is reduced, and by promoting footwall collapse local accommodation was formed, preventing the delivery of large quantities of sediment to the adjacent basin. The limited sediment supply, combined with the presence of relatively short-lived segment linkage points along the rift flanks (e.g. relay ramps; Gawthorpe et al., 1993; Leeder & Jackson, 1993; Eliet & Gawthorpe, 1995; Densmore et al., 2003; 2004; Elliott et al., 2012; Zhong & Escalona 2020) prevented the development of large, long-lived sedimentary systems in the Gimsan Basin. This interpretation is supported by well data, which indicate that although present, turbidites are rare and volumetrically small.

The topography and thus accommodation within the Gimsan Basin were controlled by its underlying structural template which, in this salt-influenced rift, was largely defined by a series of rather subtle topographic highs and lows, rather than discrete, fault-bounded depocentres usually found in salt-free rifts. One potential cause for this structural configuration was the distribution of the deeper structures over the study area. In the north of the study area, where the BFC borders the Gimsan Basin, three normal faults that offset the top of the evaporite sequence are imaged (Figure 4a). In contrast, to the south, where the VFC borders the basin, only two such structures are imaged (Figure 4b). The presence of the additional fault in the north meant that extension was distributed over three structures rather than two, resulting in two shallower sub-basins rather than, as observed in the south, one relatively deep half-graben (Figures 4 & 11). The spatial distribution and NE-SW orientation of these deeper structures has been used to suggest a Caledonide origin for these structures (Doré et al., 1997). Bunkholt et al., (2021) suggest that the late Permian – Early Triassic rift event exploited these older trends and that this control continued through to the Late Jurassic rifting. These deep-seated structures controlled not only the geometry of the Gimsan Basin, but also the larger-scale topographic evolution of the rift flanking fault systems, with the evaporite controlling the smaller, footwall-scale development. This had important implications for sediment delivery to the rift axis.

8.3. Comparison with other rift basins

We show that the presence of the pre-rift salt layer on the Halten Terrace strongly controlled its tectono-stratigraphic evolution. Salt is present in a number of other basins globally with pre-, syn- and post-rift salt layers controlling the structural and sedimentary fill (Rowan 2014). The majority of well-documented salt provinces (e.g. the northern Gulf of Mexico, the Aptian salt basins offshore Brazil, the Lower Congo and Kwanza basins offshore West Africa) are presently on passive margins that contain end syn-rift-to-early post-rift salt. In these settings, sediment loading or basin tilting drives salt flow that controls the post-rift evolution of the related basins (Rowan 2014).

In comparison to passive margin salt basins, there are relatively few well-documented examples of pre-rift salt layer impacting the syn-rift tectono-stratigraphic evolution of a rift system. Salt-influenced rift basins are however found in NW Europe, where the Lopingian (Upper Permian) Zechstein Supergroup evaporite succession has acted as a major intra-stratal detachment and decoupled sub- and supra-salt strain during multiple rift phases; and flowed to create diapiris and minibasins (e.g., Stewart et al., 1997; Clark et al., 1998; Jackson & Lewis 2013; Jackson et al., 2019). The Halten Terrace differs from the North Sea rift system in two key ways: (i) the evaporite unit in the Halten Terrace is relatively thin (< 500 m) and was much less mobile (i.e., it was likely halite-poor), thus was not associated with major diapirism; and (ii) the salt only experienced a single (rather than multiple) rift event.

The lateral facies and thickness variation seen within the Zechstein Supergroup mean that certain parts of the unit, in particular where it is relatively thin and halite-poor, such as at the basin flanks, may be analogous to the Halten Terrace. Duffy et al., (2012) study one such basin flank in the eastern Danish Central Graben, showing that along-strike (relative to fault strike) thickening of the Zechstein Supergroup was associated with increased diapirism of the unit, and an associated change from rift- to salt-related structural styles. For example, an overall half-graben geometry in the salt-poor north of their study area was controlled by a single, large, basin-bounding normal fault, comparable to the VFC; in contrast, in the salt-rich southern part of the basin, accommodation generation was more complex due to the growth of salt structures (i.e., diapir) and faults, broadly similar to that seen along the BFC. Similar structural variations are seen in the Channel Basin of southern England, where the Triassic Mercia Mudstone evaporite succession played a major role in the Jurassic-Cretaceous rift evolution of the overlying Wessex Basin (Stewart et al., 1996; Harvey & Stewart 1998). Although inverted during the Cenozoic, seismic and well data show that the Jurassic-Cretaceous syn-rift structural evolution was controlled by the thickness variations of the Triassic salt layer detaching the basement faults from those of the overlying rift system (Harvey & Stewart 1998).

These studies clearly show that the degree of linkage between basement and cover faults is linked to the thickness and facies of the salt layer that separates the two fault populations. However, the impact of this structural evolution on the stratigraphic evolution of the rift systems is considered in these studies, principally because of a lack of well data to constrain the sedimentology and stratigraphic of the coeval syn-rift succession. The present study documents not only along-strike variations in the structural evolution of a rift flank under varying degrees of salt control, but also the impact this variable evolution has had on the stratigraphic evolution of the hangingwall depocentre. A broad zone of rift-flank deformation strongly segments the basin floor, complicating sediment dispersal patterns; such complexity is not reported in rift systems lacking salt-influenced rifting or captured in related models (Gawthorpe & Leeder, 2000). The absence of well-developed drainage catchments establishing long-lived sediment source areas and pathways may be also be due to the small-scale of the structures along the border fault complexes. Due to the sliding on the salt unit, the footwall cover will become increasingly segmented into small fault blocks, thus any catchments that did form would be small and able to supply only minor volumes of sediment to the hangingwall basin.

9. Conclusions

1. The structural style changes along the eastern flank of the Halten Terrace, offshore Mid-Norway from the Bremstein Fault Complex in the north where a breached monocline produced a series of horst and grabens further south strain progressively became more localised onto a single, through-going structure with footwall collapse along the Vingleia Fault Complex. The change in structural style is closely related to the presence of a pre-rift evaporite layer which acts as a detachment with syn-rift faults soling out into it and decouples structure above and below it.

2. The Bremstein Fault Complex underwent limited footwall uplift throughout the syn-rift period with relatively small-scale, localised erosion of footwall blocks supplying limited volumes of sediment downdip. Although volumetrically small, erosion of sandstone-dominated succession combined with complex structural topography of the Bremstein Fault Complex promoted the accumulation of clastic-rich localised depocentres hosted within the fault complex.

3. The Vingleia Fault Complex has undergone extensive footwall erosion combined with a phase of structural collapse. Erosion has resulted from two periods of footwall uplift, rotation and sub-aerial exposure promoting erosion followed by a later period of footwall collapse with block sliding on the Triassic evaporite layer. This erosion supplied sediment to both the Gimsan Basin and the adjacent hangingwall dipslope with a shoreface succession found on the flanks of the dipslope.

4. The Gimsan Basin was largely underfilled with little sediment supply from rift flanks or cross-shelf antecedent supplies. Small scale submarine fans were however, sourced from the fault scarp erosion along Vingleia Fault Complex although syn-rift sedimentation was predominantly pelagic/hemi-pelagic with occasional mud-dominated submarine slide sourced from rift flank collapse.

5. The variations in rift flank structural style have a profound influence on the sediment pathways, volumes and facies of the syn-rift sediment delivered to the evolving rift basin downdip. In contrast to basins that developed without a pre-rift evaporate layer, the variable topography along the rift flanks controlled by evaporate-influenced structural evolution facilitate local sediment supply along with small, localised accommodation space which means that syn-rift sediment accumulation will be localised along the rift flank with limited supply deeper into the rift basin.

6. Where through-going structures develop along the rift flanks, the presence of evaporite facies also will suppress the footwall topographic expression, through footwall collapse facilitated by evaporite detachment, limiting the amount of sediment supply to the basins downdip.

10. Acknowledgements

Statoil (Now Equinor) ASA are thanked for providing funding and data for the **S**alt **I**nfluenced **R**ift **B**asins project at Imperial College, University of Manchester and the University of Bergen. We would like to thank Fugro MCS for permission to use and to publish the seismic data illustrated in Figures 1 & 4. We would like to thank in particular the members of the Equinor Norwegian Sea Shallow Water Exploration Team in Harstad and the Equinor Research Centre in Bergen for their help and assistance with this work. We would also like to thank Schlumberger for providing *Petrel* to Imperial College, University of Manchester and University of Bergen. Basin Research Associate Editor Wonsuck Kim, reviewers Adrian Hartley, Stefano Tavani and an anonymous reviewer are thanked for their constructive reviews which have improved the quality of the paper.

REFERENCES

Bell, R.E., Jackson, C., Elliott, G.M., Gawthorpe, R.L., Sharp, I.R. & Michelsen, L 2014. Insight into the development of major rift-related unconformities from geologically constrained subsidence modelling: Halten Terrace, offshore Mid Norway. Basin Research. 26, 203- 224.

Bilal, A., McClay, K.R & Scarselli, N. (2018) Fault-scarp degradation in the central Exmouth Plateau, North West Shelf, Australia In: Passive Margins: Tectonics, Sedimentation and Magmatism (Ed. by McClay, K.R. & Hammerstein, J.A.) **476**, 231-257. Geological Society, London, Special Publications.

Blystad, P., Brekke, H., Faerseth, R.B., Larsen, B.T., Skogseid, J. & Torudbakken, B. (1995) Structural Elements of the Norwegian Continental Shelf: Part Ii the Norwegian Sea Region. **NPD Bulletin No 8**.

Brekke, H. (2000) The Tectonic Evolution of the Norwegian Sea Continental Margin with Emphasis on the Vøring and Møre Basins. *Geological Society, London, Special Publications*, **167,** 327-378.

Bunkholt, H.S.S., Oftedal, B.T., Hansen, J.A., Løseth, H. & Kløvjan, O.S. 2021. Halten–Dønna Terraces & Trøndelag Platform Composite Tectono-Sedimentary Element, offshore Mid-Norway. In: S. S. Drachev, H. Brekke, E. Henriksen, T. Moore (eds). Sedimentary successions of the Arctic Region and their hydrocarbon prospectivity. Geological Society, London, Memoirs, 57

Bukovics, C., Cartier, E.G., Shaw, N.D. & Ziegler, P.A. (1984) Structure and Development of the Mid-Norway Continental Margin. In: *Petroleum Geology of the North European Margin* (Ed. by A. M. Spencer), 407 - 423. Graham & Trotman, London.

Clark, J.A., Stewart, S.A. & Cartwright, J. (1998) Evolution of the NW Margin of the North Permian Basin, UK North Sea. *Journal of the Geological Society* **155,** 663-676.

Coleman, A.J., Duffy, O.B. & Jackson, C.A-L. (2019) Growth folds above propagating normal faults. *Earth-Science Reviews*, 196, 102885

Corfield, S. & Sharp, I.R. (2000) Structural Style and Stratigraphic Architecture of Fault Propagation Folding in Extensional Settings: A Seismic Example from the Smørbukk, Halten Terrace, Mid Norway. *Basin Research*, **12,** 329-341.

Corfield, S., Sharp, I., Häger, K.-O., Dreyer, T., Underhill, J., Ole, J.M. & Tom, D. (2001) An Integrated Study of the Garn and Melke Formations (Middle to Upper Jurassic) of the Smorbukk Area, Halten Terrace, Mid-Norway. In: *Norwegian Petroleum Society Special Publications* (Ed. by, Martinsen, O.J & Dreyer, T.) **Volume 10**, 199-210. Elsevier.

DALLAND, A., WORSLEY, D. & OFSTAD, K. (1988) A Lithostratigraphic Scheme for the Mesozoic and Cenozoic Succession Mid - and Northern Norway, Norwegian Petroleum Directorate. **NPD Bulletin No 4**.

DENSMORE, A.L., DAWERS, N.H., GUPTA, S., ALLEN, P.A. & GILPIN, R. (2003) Landscape Evolution at Extensional Relay Zones. *Journal of Geophysical Research*, **108,** 2273.

DENSMORE, A.L., DAWERS, N.H., GUPTA, S., GUIDON, R. & GOLDIN, T. (2004) Footwall Topographic Development during Continental Extension. *Journal of Geophysical Research*, **109,** F03001.

DOOLEY, T., MCCLAY, K.R. & PASCOE, R. (2003) 3d Analogue Models of Variable Displacement Extensional Faults: Applications to the Revfallet Fault System, Offshore Mid-Norway. In: *New Insights into Structural Interpretation and Modelling* (Ed. by D. A. Nieuwland), **212**, 151-167. Geological Society, London, Special Publications.

DORÉ, A.G., LUNDIN, E.R., JENSEN, L.N., BIRKELAND, O., ELIASSEN, P.E. & FICHLER, C. (1999) Principal Tectonic Events in the Evolution of the Northwest European Atlantic Margin. In: *Petroleum Geology of Northwest Europe: Proceedings of the 5th Conference* (Ed. by A. J. Fleet & S. A. R. Boldy), 41-61. Geological Society.

DUFFY**,** O.B., GAWTHORPE, R.L, DOCHERTY M & BROCKLEHURST S. H. Mobile evaporite controls on the structural style and evolution of rift basins: Danish Central Graben, North Sea (2013) Basin Research, 25, 310 - 330

DORE, A.G., LUNDIN, E.R., BIRKELAND, O., ELIASSEN, P.E. & JENSEN, L.N. (1997) The NE Atlantic Margin; Implications of Late Mesozoic and Cenozoic Events for Hydrocarbon Prospectivity. *Petroleum Geoscience*, **3,** 117-131.

EHRLICH, R. & GABRIELSEN, R.H. (2004) The Complexity of a Ramp-Flat-Ramp Fault and Its Effect on Hanging-Wall Structuring: An Example from the Njord Oil Field, Offshore Mid-Norway. *Petroleum Geoscience*, **10,** 305-317.

ELIET, P.P. & GAWTHORPE, R.L. (1995) Drainage Development and Sediment Supply within Rifts, Examples from the Sperchios Basin, Central Greece. *Journal of the Geological Society*, **152,** 883-893.

ELLIOTT, G.M., WILSON, P., JACKSON, C.A.L., GAWTHORPE, R.L., MICHELSEN, L. & SHARP, I.R. (2012) The Linkage between Fault Throw and Footwall Scarp Erosion Patterns: An Example from the Bremstein Fault Complex, Offshore Mid-Norway. *Basin Research*, **24,** 180-197.

ELLIOTT, G.M., WILSON, P., JACKSON, C.A.L., GAWTHORPE, R.L., MICHELSEN, L. & SHARP, I.R. (2017) Late syn-rift evolution of the Vingleia Fault Complex, Halten Terrace, offshore Mid-Norway; a test of rift basin tectono-stratigraphic models. *Basin Research*, 29 (Suppl. 1) 465- 487.

GAWTHORPE, R.L. & HURST, J.M. (1993) Transfer Zones in Extensional Basins: Their Structural Style and Influence on Drainage Development and Stratigraphy. *Journal of the Geological Society*, **150,** 1137-1152.

FALEIDE, J.I, TSIKALAS, F., BREIVIK, A.J., MJELDE, R., RITZMANN, O., ENGEN, Ø., WILSON, J. & ELDHOLM, O. (2008) Structure and evolution of the continental margin off Norway and the Barents Sea. Episodes, 31 (1), 82 - 91

GAWTHORPE, R.L., FRASER, A.J. & COLLIER, R.E.L. (1994) Sequence Stratigraphy in Active Extensional Basins: Implications for the Interpretation of Ancient Basin-Fills. *Marine and Petroleum Geology*, **11,** 642-658.

GAWTHORPE, R.L. & LEEDER, M.R. (2000) Tectono-Sedimentary Evolution of Active Extensional Basins. *Basin Research*, **12,** 195-218.

GJELLBERG, J., DREYER, T., HOIE, A., TJELLAND, T. & LILLENG, T. (1987) Late Triassic to Mid- Jurassic Sandbody Development on the Barents and Mid-Norwegian Shelf. In: *Petroleum Geology of North West Europe* (Ed. by J. Brooks & K. W. Glennie), 1105-1129. Graham & Trotman, London.

HARVEY, M.J., & STEWART, S.A., (1998) Influence of salt on the structural evolution of the Channel Basin. In: *Development, Evolution and Petroleum Geology of the Wessex Basin.* (Ed. by Underhill, J.R.) Geological Society Special Publication, 133, 241-266

HESTHAMMER, J. & FOSSEN, H. (1999) Evolution and geometries of gravitational collapse structures with examples from the Statfjord Field, northern North Sea. Marine and Petroleum Geology, 16, 259-281

JACKSON, C.A.L., LARSEN, E., HANSLIEN, S. & TJEMSLAND, A.-E. (2011) Controls on Synrift Turbidite Deposition on the Hanging Wall of the South Viking Graben, North Sea Rift System, Offshore Norway. *AAPG Bulletin*, **95,** 1557-1587.

JACKSON,C.A-L & LEWIS, M.M. (2014) Structural style and evolution of a salt-influenced rift basin margin; the impact of variations in salt composition and the role of polyphase extension Basin Research, 26, 81 - 102

JACKSON, C.A-L., ELLIOTT, G.M., ROYCE-ROGERS, E., GAWTHORPE, R.L. & AAS, T.E. (2019) Salt thickness and composition influence rift structural style, northern North Sea, offshore Norway. *Basin Research* 31 (3), 514 – 538

JONES, G.E.D., WELBON, A.I.F., MOHAMMADLOU, H., SAKHAROV, A., FORD, J. NEEDHAM, T. & OTTESEN, C. (2021) Complex stratigraphic fill of a small, confined syn-rift basins: an Upper Jurassic example from offshore Mid-Norway In: Cross-Border Themes in Petroleum Geology II: Atlantic Margin and Barents Sea (Ed. by D. Chiarella, D., Archer, S.G., Howell, J.A., Jackson, C.A.-L., Kombrink, H. & Patruno, S.), Geological Society Special Publication, 495,

KANE, K.E., JACKSON, C.A.-L. & LARSEN, E. (2010) Normal fault growth and fault-related folding in a salt-influenced rift basin: south Viking Graben, offshore Norway. *Journal of Structural Geology*, 32, 490–506.

JACOBSEN, V.W. & VAN VEEN, P. (1984) The Triassic Offshore Norway North of 62n. In: *Petroleum Geology of the North European Margin* (Ed. by A. M. Spencer), 317-327. Graham & Trotman.

LEEDER, M.R. & JACKSON, J.A. (1993) The Interaction between Normal Faulting and Drainage in Active Extensional Basins, with Examples from the Western United States and Central Greece. *Basin Research*, **5,** 79-102.

MCLEOD, A.E. & UNDERHILL, J.R. (1999) Processes and Products of Footwall Degradation, Northern Brent Field, Northern North Sea. In: *Petroleum Geology of Northwest Europe: Proceedings of the 5th Conference* (Ed. by A. J. Fleet & S. A. R. Boldy), *Geological Society, London,* 91-106.

MARSH, N., IMBER, J., HOLDSWORTH, R.E., BROCKBANK, P. & RINGROSE, P. (2010) The Structural Evolution of the Halten Terrace, Offshore Mid-Norway: Extensional Fault Growth and Strain Localisation in a Multi-Layer Brittle & Ductile System. *Basin Research*, **22,** 195-214.

MARTINIUS, A.W., KAAS, I., NSS, A., HELGESEN, G., KJREFJORD, J.M., LEITH, D.A., OLE, J.M. & TOM, D. (2001) Sedimentology of the Heterolithic and Tide-Dominated Tilje Formation (Early Jurassic, Halten Terrace, Offshore Mid-Norway). In: *Norwegian Petroleum Society Special Publications* (Ed. by Martinsen, O.J & Dreyer, T.) **Volume 10**, 103-144. Elsevier.

MARTINIUS, A.W., RINGROSE, P.S., BROSTROM, C., ELFENBEIN, C., NAESS, A. & RINGAS, J.E. (2005) Reservoir Challenges of Heterolithic Tidal Sandstone Reservoirs in the Halten Terrace, Mid-Norway. *Petroleum Geoscience*, **11,** 3-16.

MESSINA, C., NEMEC, W., MARTINIUS, A.W. & ELFENBEIN, C. (2014) The Garn Formation (Bajocian-Bathonian) in the Kristin Field, Halten Terrace: its origin, facies architecture and primary heterogeneity model In: *From Depositional Systems to Sedimentary Successions on the Norwegian Continental Margin* (Ed. by Martinius, A.W., Ravnås, R., Howell, J.A. & Wonham, J.P.) 513 – 550. International Association of Sedimentologists/John Wiley & Sons, Ltd

NØTTVEDT, A., BERGE, A.M., DAWERS, N.H., FÆRSETH, R.B., HÄGER, K.O., MANGERUD, G. & PUIGDEFABREGAS, C. (2000) Syn-Rift Evolution and Resulting Play Models in the Snorre-H Area, Northern North Sea. *Geological Society, London, Special Publications*, **167,** 179-218.

PASCOE, R., HOOPER, P.R., STORHAUG, K. & HARPER, H. (1999) Evolution of Extensional Styles at the Southern Termination of the Nordland Ridge, Mid-Norway: A Response to Variations in Coupling above Triassic Salt. In: *Petroleum Geology of Northwest Europe: Proceedings of the 5th Conference* (Ed. by J. A. Fleet & S. A. R. Boldy), 83-90. Geological Society of London.

PERON-PINVIDIC, G & OSMUNDSEN, P.T. (2018) The Mid Norwegian - NE Greenland conjugate margins: Rifting evolution, margin segmentation, and breakup. *Marine and Petroleum Geology*, 98, 162-184

PENGE, J., TAYLOR, B., HUCKERBY, J.A. & MUNNS, J.W. (1993) Extension and Salt Tectonics in the East Central Graben. In: *Petroleum Geology of Northwest Europe: Proceedings of the 4th Conference* (Ed. by J. R. Parker), 1197-1209. Geological Society of London, London.

PROSSER, S. (1993) Rift-Related Linked Depositional Systems and Their Seismic Expression. In: *Tectonics and Seismic Sequence Stratigraphy* (Ed. by G. D. Williams & A. Dobb), **71**, 35-66. Geological Society, London, Special Publications.

PROVAN, D. (1992) Draugen Oil Field, Haltenbanken Province, Offshore Norway. In: *Giant Oil and Gas Fields of the Last Decade 1978-1988* (Ed. by M. T. Halbouty), **AAPG Memoir 54**, 371-382. AAPG, Tulsa.

RAVNAS, R. & STEEL, R.J. (1998) Architecture of Marine Rift-Basin Successions. *AAPG Bulletin*, **82,** 110-146.

RAVNÅS, R., NØTTVEDT, A., STEEL, R.J. & WINDELSTAD, J. (2000) Syn-Rift Sedimentary Architectures in the Northern North Sea. In: *Dynamics of the Norwegian Margin* (Ed. by A. Nottvedt), **167**, 133-177. Geological Society, London, Special Publications.

ROBERTS, A.M., KUSZNIR, N.J., YIELDING, G. & BEELEY, H. (2019) Mapping the bathymetric evolution of the Northern North Sea: from Jurassic synrift archipelago through Cretaceous–Tertiary post-rift subsidence. *Petroleum Geoscience*, 25, 306-321.

ROWAN, M.G. (2014) Passive-margin salt basins: hyperextension, evaporite deposition, and salt tectonics. *Basin Research*, 26, 154-182

RICHARDSON, N.J., UNDERHILL, J.R. & LEWIS, G. (2005) The Role of Evaporite Mobility in Modifying Subsidence Patterns During Normal Fault Growth and Linkage, Halten Terrace, Mid-Norway. *Basin Research*, **17,** 203-223.

ROBERTS, A.M. & YIELDING, G. (1991) Deformation around basin-margin faults in the North Sea/mid-Norway rift In: The Geometry of Normal Faults (Ed. by Roberts, A.M., Yielding, G. & Freeman, B.), **56,** 61 – 78, Geological Society Special Publication, London

ROBERTS, D.G., THOMPSON, M., MITCHENER, B., HOSSACK, J., CARMICHAEL, S. & BJORNSETH, H.M. (1999) Palaeozoic to Tertiary Rift and Basin Dynamics: Mid-Norway to the Bay of Biscay - a New Context for Hydrocarbon Prospectivity in the Deep Water Frontier. In: *Petroleum Geology of Northwest Europe* (Ed. by J. A. Fleet & S. A. R. Boldy), 7-40. Geological Society of London.

SANDWELL, D.T. & SMITH, W.H.F. (1997) Marine Gravity Anomaly from Geosat and Ers 1 Satellite Altimetry. *Journal of Geophysical Research*, **102,** 10039-10054.

STEWART, S.A., RUFFELL, A.H. & HARVEY, M.J. (1997) Relationship between basement-linked and gravity-driven fault systems in the UKCS salt basins. *Marine and Petroleum Geology*, 14, 581–604.

STEWART, S.A., HARVEY, M.J., OTTO, S.C. & WESTON, P.J. (1996) Influence of salt on fault geometry; example from the UK salt basins. In: *Salt Tectonics* (Ed by Alsop, G.I., Blundell, D.J. & Davison, I.) Geological Society Special Publication, 100, 175-202

SLAGSTAD, T., DAVIDSEN, B. & DALY, J.S. (2011) Age and Composition of Crystalline Basement Rocks on the Norwegian Continental Margin: Offshore Extension and Continuity of the Caledonian–Appalachian Orogenic Belt. *Journal of the Geological Society*, **168,** 1167-1185.

SWIECICKI, T., GIBBS, P.B., FARROW, G.E. & COWARD, M.P. (1998) A Tectonostratigraphic Framework for the Mid-Norway Region. *Marine and Petroleum Geology*, **15,** 245-276.

TAVANI, S. & GRANADO, P. (2015) Along-strike evolution of folding, stretching and breaching of supra-salt strata in the Plataforma Burgalesa extensional forced fold system (northern Spain) *Basin Research*, 27 (4), 573 – 585.

TAVANI, S., BALSAMO, F. & GRANADO, P. (2018) Petroleum system in supra-salt strata of extensional forced-folds: A casestudy from the Basque-Cantabrian basin (Spain) *Marine and Petroleum Geology*, 96, 315 - 330

UNDERHILL, J.R., SAWYER, M.J., HODGSON, P., SHALLCROSS, M.D. & GAWTHORPE, R.L. (1997) Implications of Fault Scarp Degradation for Brent Group Prospectivity, Ninian Field, Northern North Sea. *AAPG Bulletin*, **81,** 999-1022.

WELBON, A.I.F., BROCKBANK, P.J., BRUNSDEN, D. & OLSEN, T.S. (2007) Characterizing and Producing from Reservoirs in Landslides: Challenges and Opportunities. In: *Structurally Complex Reservoirs* (Ed. by S. J. Jolley, D. Barr, J. J. Walsh & R. J. Knipe), **292**, 49-74. Geological Society Special Publication, London.

WILSON, P., ELLIOTT, G.M., GAWTHORPE, R.L., JACKSON, C.A.L., MICHELSEN, L.M. & SHARP, I.R. (2013) Structure and Growth of an Evaporite-Detached Normal Fault Array: The Southern Bremstein Fault Complex, Offshore Mid-Norway. *Journal of Structural Geology*, 51, 74 - 91

WILSON, P., ELLIOTT, G.M., GAWTHORPE, R.L., JACKSON, C.A.-L. & SHARP, I.R. (2015) Lateral variation in structural style along an evaporite-influenced rift fault system in the Halten Terrace, Norway: the influence of basement structure and evaporite facies. Journal of Structural Geology, 79, 10–123.

WITHJACK, M.O., MEISLING, K. & RUSSELL, L. (1989) Forced Folding and Basement-Detached Normal Faulting in the Haltenbanken Area, Offshore Norway. In: *Extensional Tectonics and Stratigraphy of the North Atlantic Margins* (Ed. by A. Tankard & H. R. Balkwill), **AAPG Memoir 46**, 567-575. AAPG.

Withjack, M.O., Olson, J. & Peterson, E. (1990) Experimental Models of Extensional Forced Folds. *AAPG Bulletin*, **74,** 1038-1054.

Withjack, M.O., Schlische, R.W. & Olsen, P.O. (2002) Rift basin structure and its influence on sedimentary systems In: Sedimentation in Continental Rifts (Ed. by R.W. Renaut & G.M. Ashley) SEPM Special Publication 73, 57 – 81.

Yielding, G. (1990) Footwall uplift associated with Late Jurassic normal faulting in the northern North Sea. Journal of the Geological Society, 147, 219-222.

Zastrozhnov, D., Gernigon, L., Gogin, I., Planke, S., Abdelmalak, M.M., Polteau, S., Faleide, J.I., Manton, B. & Myklebust, R. (2020) Regional structure and polyphased Cretaceous-Paleocene rift and basin development of the mid-Norwegian volcanic passive margin. *Marine and Petroleum Geology*, 115, 104269

Zhong, X & Escalona, A. (2020) Evidence of rift segmentation and controls of Middle to Late Jurassic synrift deposition in the Ryggsteinen ridge area, northern North Sea AAPG Bulletin, **104**, 1531 – 1565

van der Zwan, C.J. (1990) Palynostratigraphy and Palynofacies Reconstruction of the Upper Jurassic to Lowermost Cretaceous of the Draugen Field, Offshore Mid Norway. *Review of Palaeobotany and Palynology*, **62,** 157-186.

FIGURES CAPTIONS

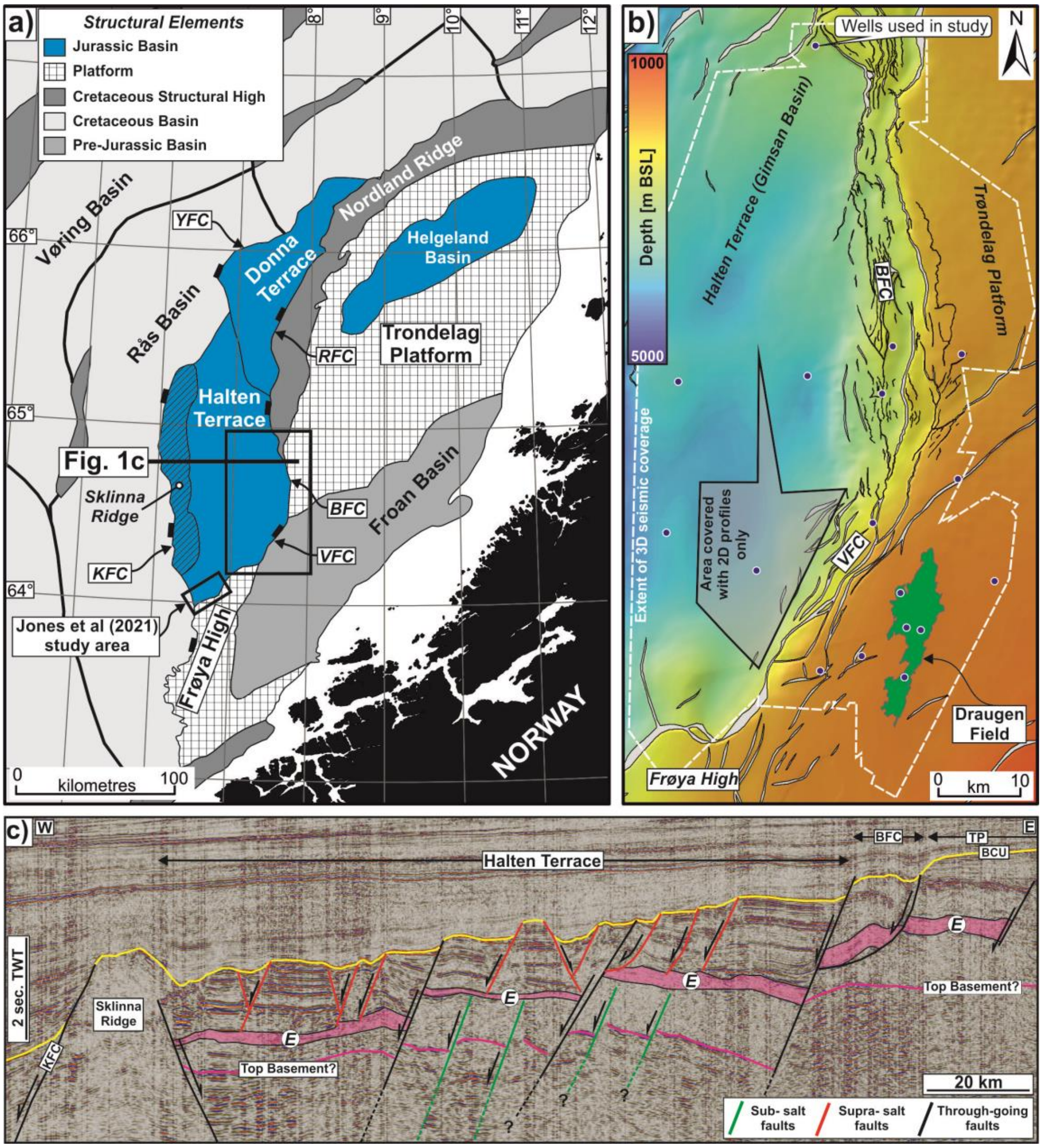

Figure 1: a) Structural elements map of the Mid-Norwegian Shelf showing the location of the Halten Terrace (modified from Blystad et al., 1998) b) Base Cretaceous Unconformity depth structure map showing the study area along the eastern flank of the Halten Terrace. The white polygon outlines the areal extent of 3D seismic reflection data used in the study with the grey polygon delimiting the region where only 2D profiles were used. The location of the wells used in the study are highlighted also along with the outline of the Draugen oil field. BFC: Bremstein Fault Complex. VFC: Vingleia Fault Complex. c) Regional seismic reflection profile across the Halten Terrace showing the influence of the evaporite upon fault distribution (see Figure 1a for location). BFC: Bremstein Fault Complex. KFC: Klakk Fault Complex. RFC: Revfallet Fault Complex TP: Trøndelag Platform. YFC: Ytreholmen Fault Complex

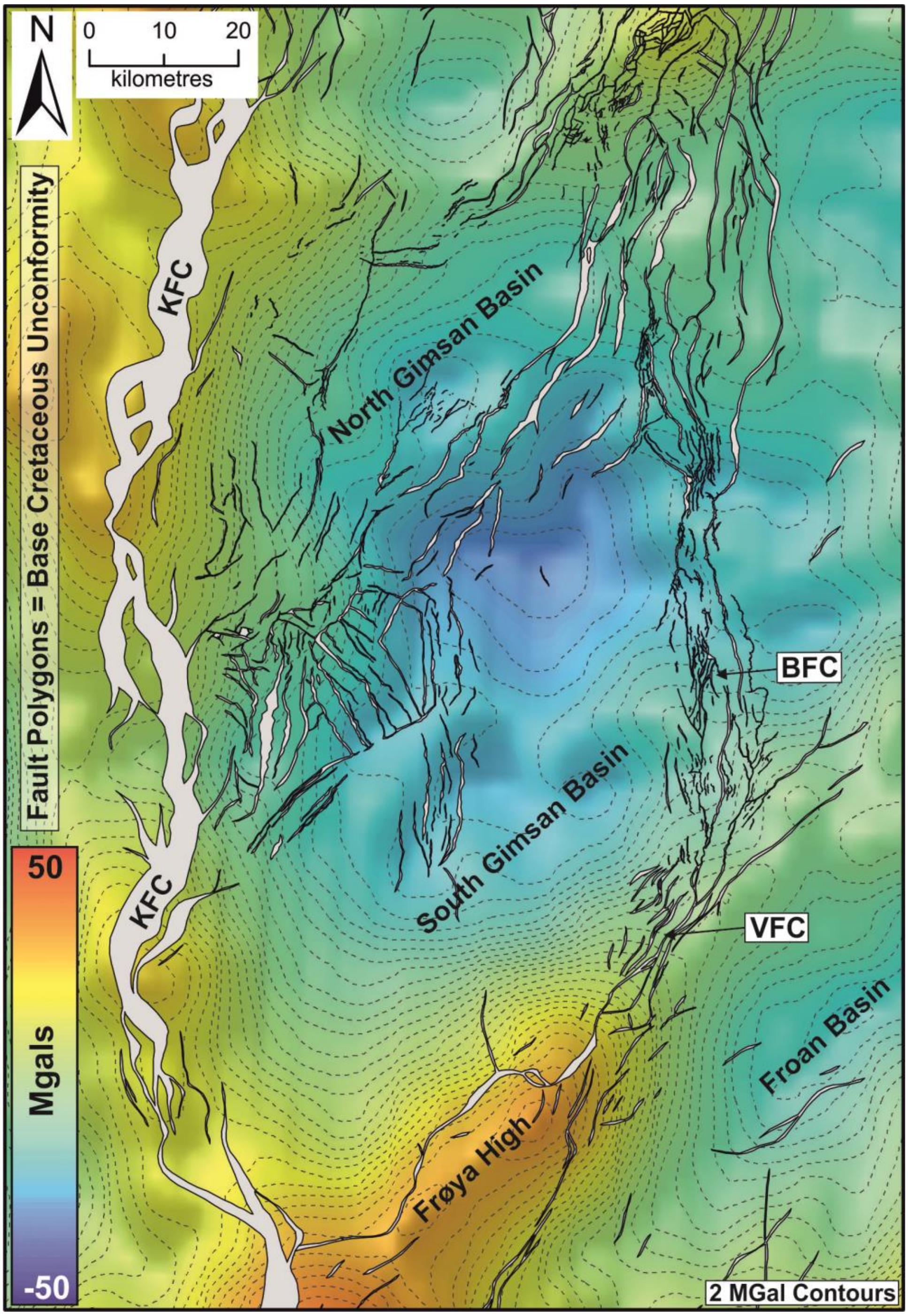

Figure 2: Free-Air gravity anomaly map based upon satellite observations (Sandwell and Smith 1997) over the Halten Terrace showing the large positive anomaly associated with the Frøya High which is bound to the north by the Vingleia Fault Complex while the Bremstein Fault Complex is associated with a gravity low. BFC: Bremstein Fault Complex. KFC: Klakk Fault Complex. VFC: Vingleia Fault Complex.

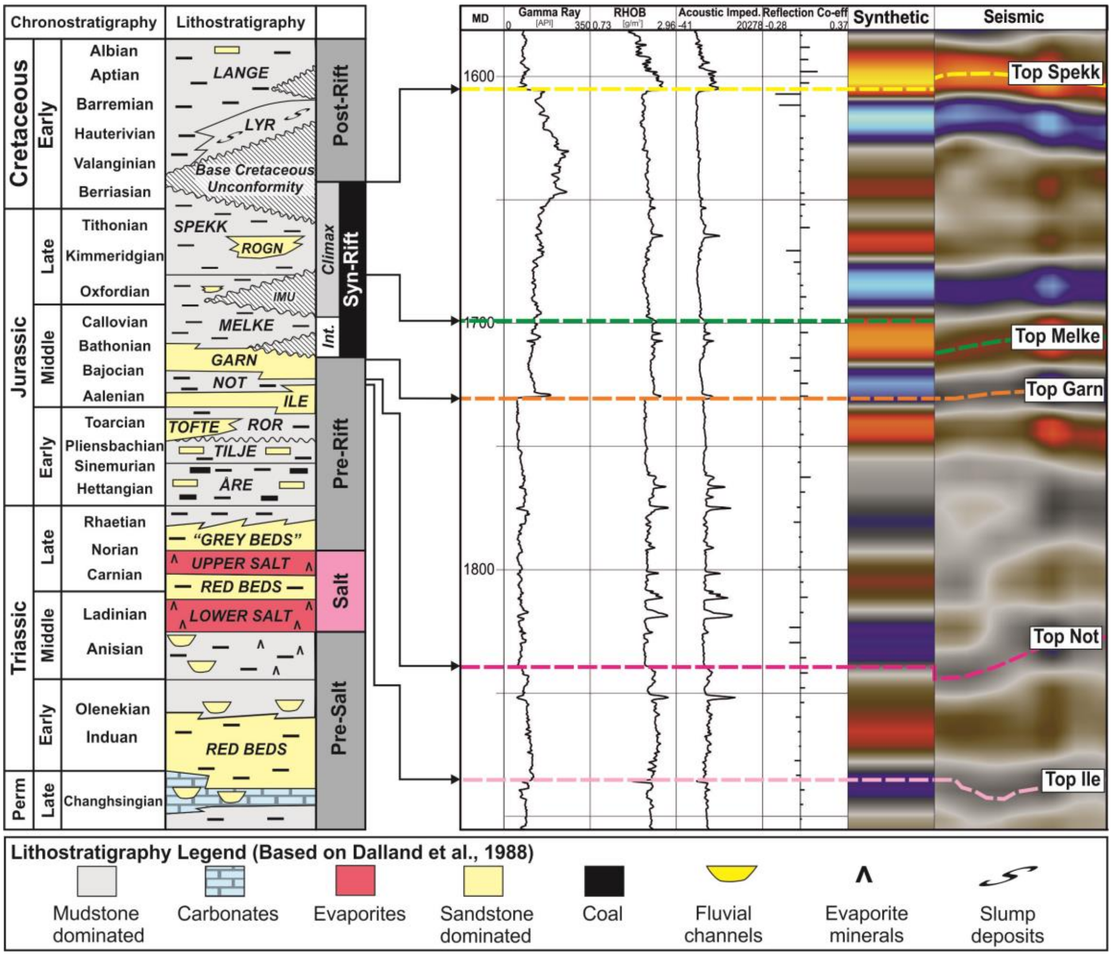

Figure 3: Stratigraphic column for the Halten Terrace based upon Dalland et al., (1988) with a synthetic seismogram for well 6407/9-8 demonstrating the correlation between the key stratigraphic markers identified in the well with seismic reflection events. IMU: Intra-Melke Unconformity

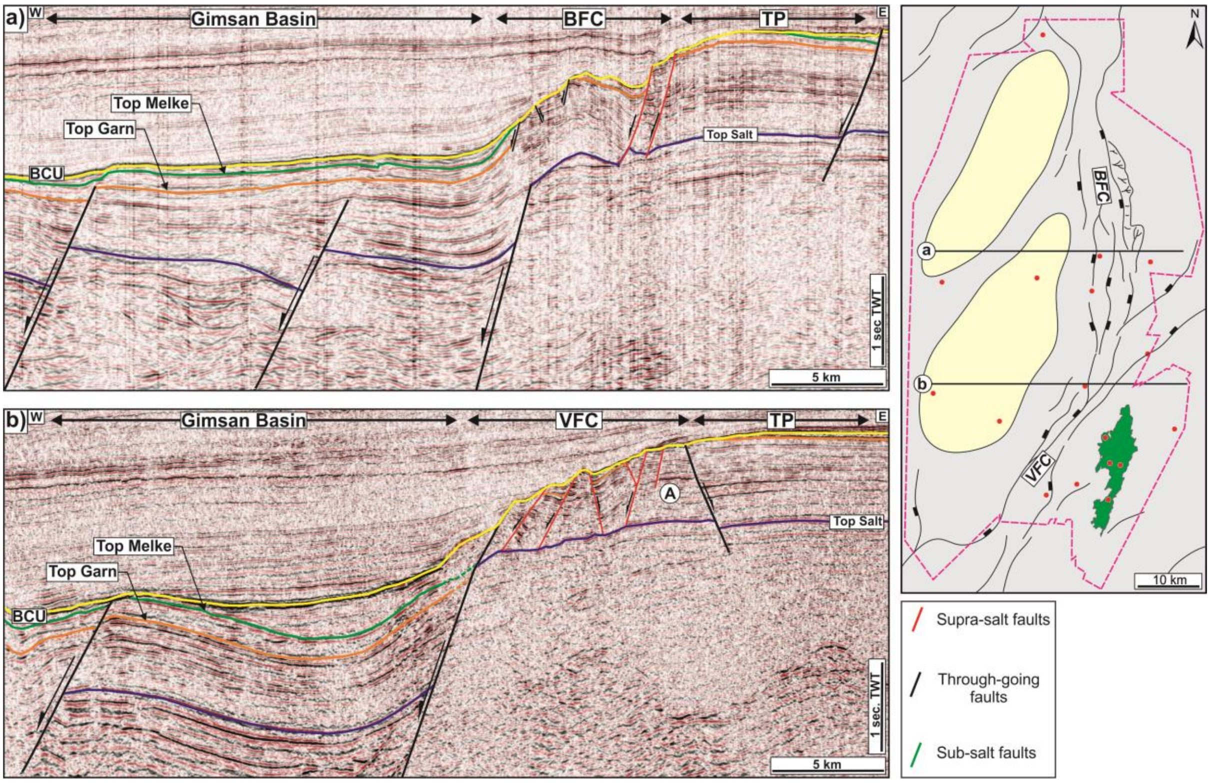

Figure 4: a) Seismic profile across Halten Terrace showing the breached monocline structure of the Bremstein Fault Complex (BFC). b) Seismic section showing the though-going structure of the Vingleia Fault Complex (VFC) along with the zone of footwall collapse along the western edge of the footwall. Fault planes are colour coded as per Figure 1c. TP: Top Evaporite.

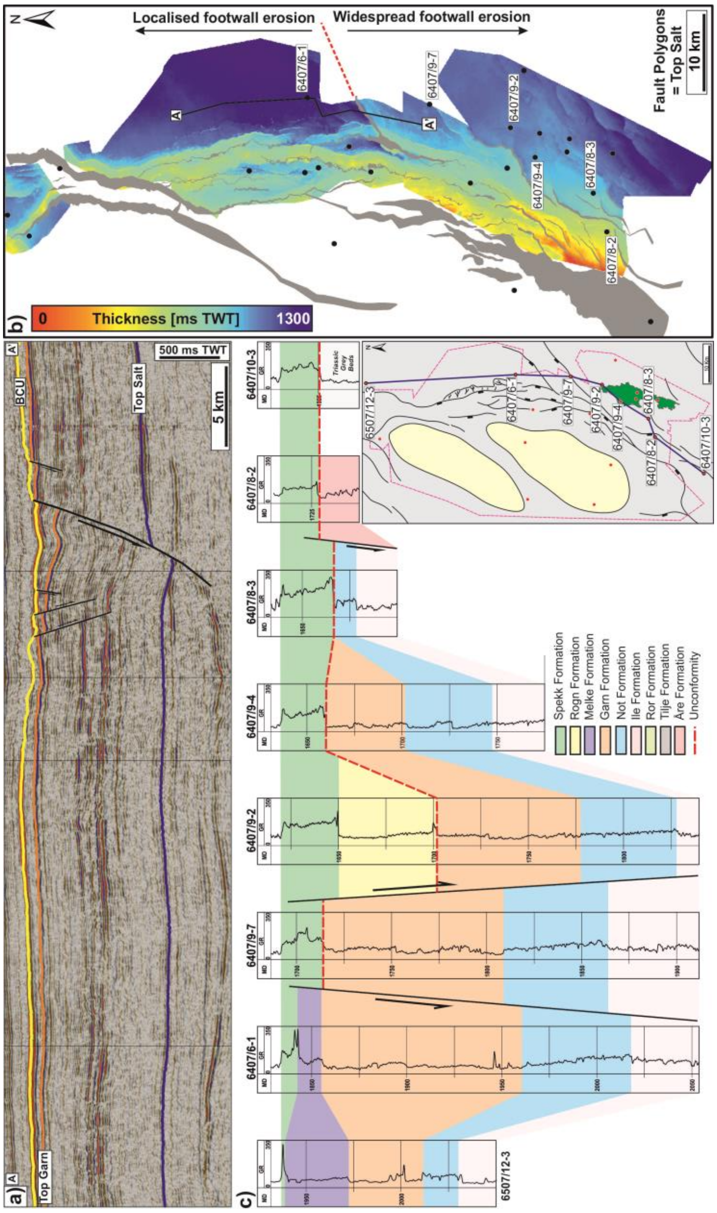

Figure 5: a) Seismic profile broadly N-S along footwall of the eastern rift flank showing a prominent NE-SW striking fault separates the rift flank into two distinct areas with widespread footwall erosion in the south and an area of more localised footwall erosion to the north. b) Top Evaporite to BCU Isochron the largest amount of footwall erosion is found in the south which progressively increases towards the VFC footwall crest whereas the BFC has a relatively uniform thickness until the reaching the fault complex itself. c) Well lithostratigraphic correlation panel along eastern rift flank showing the progressive downcutting into older footwall stratigraphy to the south. BFC: Bremstein Fault Complex. VFC: Vingleia Fault Complex.

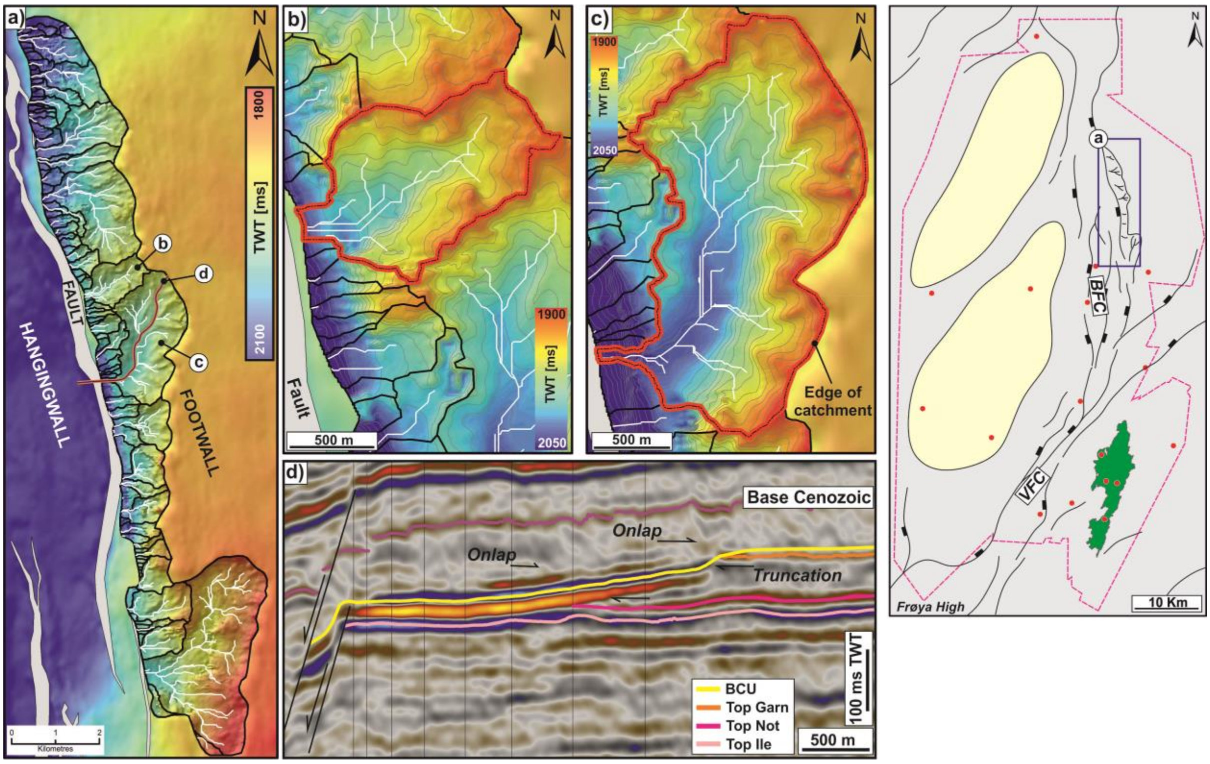

Figure 6: a) Base Cretaceous Unconformity elevation map of the BFC footwall with catchments and stream networks highlighted together with the main fault segment (in grey). b) Time structure map of linear catchment characterised by low Strahler stream order. c) Time structure map of curved catchment characterised by higher stream orders. d) Axial seismic section along footwall catchment showing the concave down incisonal nature of the system which is hosted within the sandstone-dominated Garn Formation and progressive onlap of overlying Cretaceous.

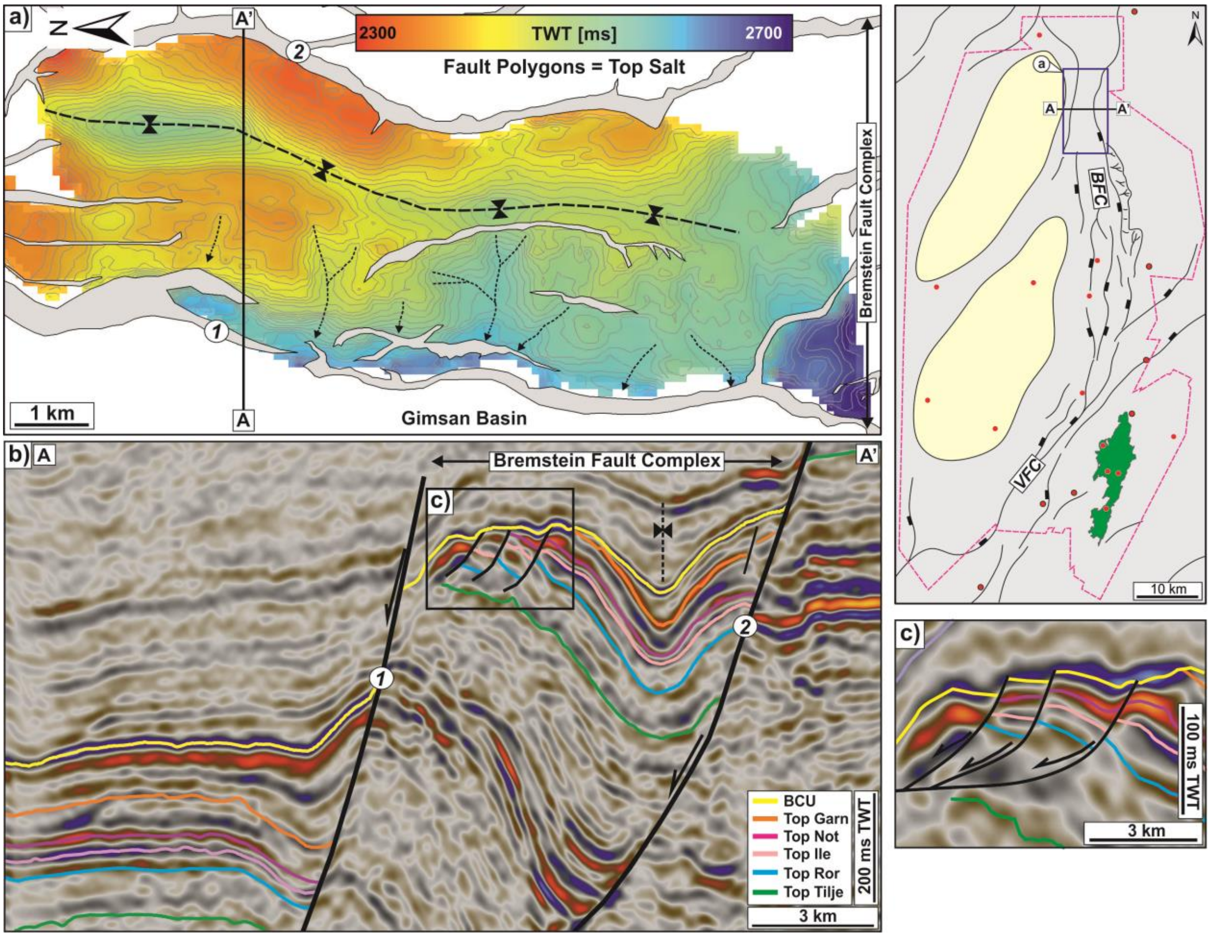

Figure 7: a) Base Cretaceous time-structure map of an individual fault block found within the Bremstein Fault Complex exhibiting a number of erosional features along the western edge of the footwall. b) Seismic profile across fault complex showing the footwall rotation that promoted crestal collapse along the crest of the footwall. c) Seismic profile highlighting footwall crestal collapse is lithologically controlled with the mudstone-dominated Ror Formation acting as a detachment for the collapse.

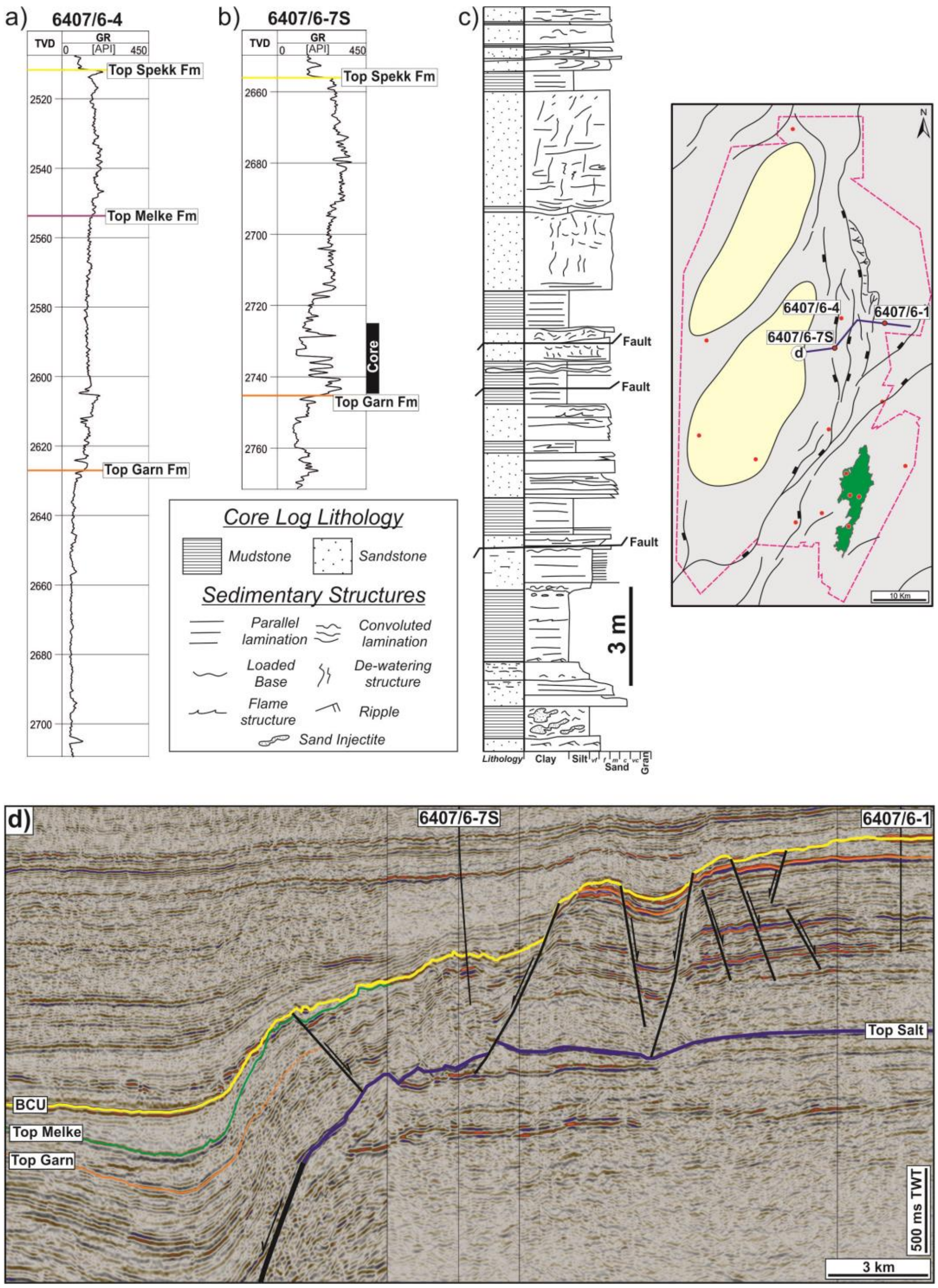

Figure 8: a) Gamma ray wireline log from well 6407/6-4 which encountered over 100 m of Melke Formation siltstone with no indication of coarse clastic lithologies. b) Gamma ray wireline log from well 6407/6-7S which encountered a 44 m thick Oxfordian sandstone package. c) 1:100 scale graphic sedimentological log from 17 m of core in well 6407/6-7S showing the presence of thick sandstone beds within the Oxfordian Melke Formation. These coarse clastic beds are thought to be derived from footwall erosion updip from the well. d) Seismic section from Trøndelag Platform across the Bremstein Fault Complex to the Gimsan Basin showing how well 6407/6-7S is hosted within the breached monocline structure.

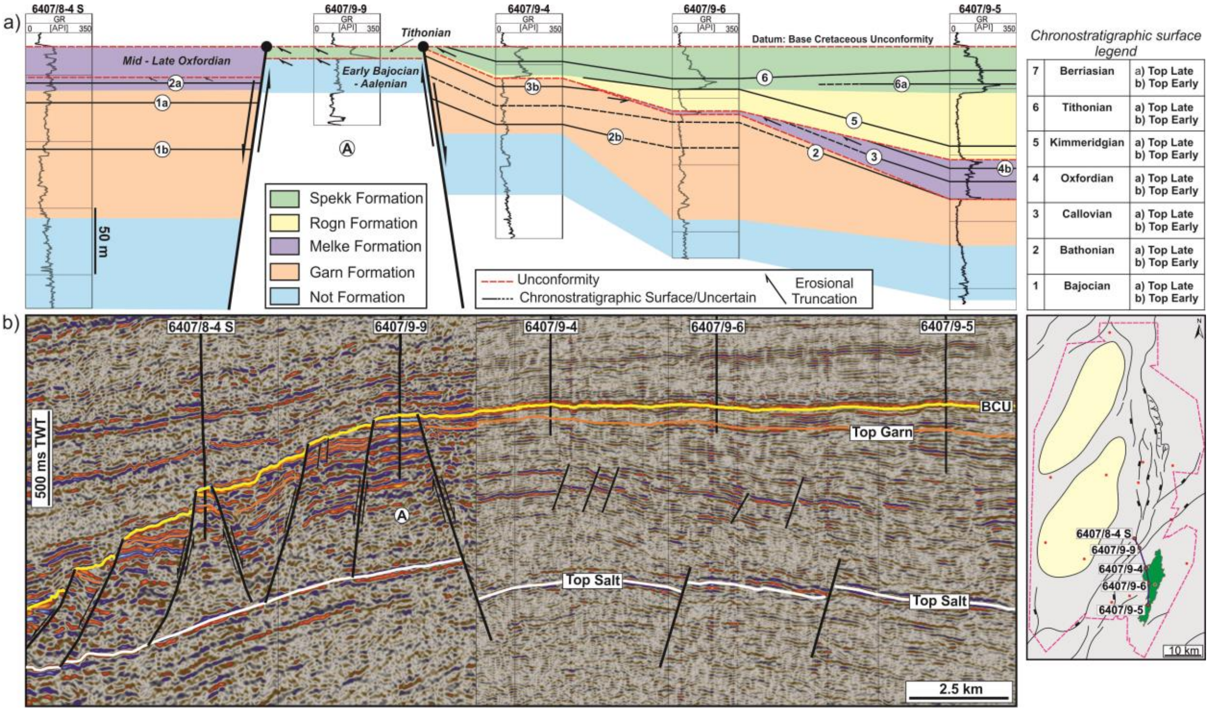

Figure 9: a) Well stratigraphic correlation of Jurassic succession along a broadly NW-SE along the footwall of the VFC. Key biostratigraphically constrained time lines are shown. The panel exhibits the progressive onlap of the Late Jurassic onto a prominent composite unconformity surface which downcuts towards the footwall crest. In addition, the perseveration of Oxfordian within the rafted block helps to constrain the timing of the footwall collapse. b) Seismic profile used to help constrain the underlying structure along the panel shown in a) and also shows the larger scale structure of the VFC footwall. Prominent horst (labelled A) delimits the easternmost limit of gravity sliding on VFC footwall.

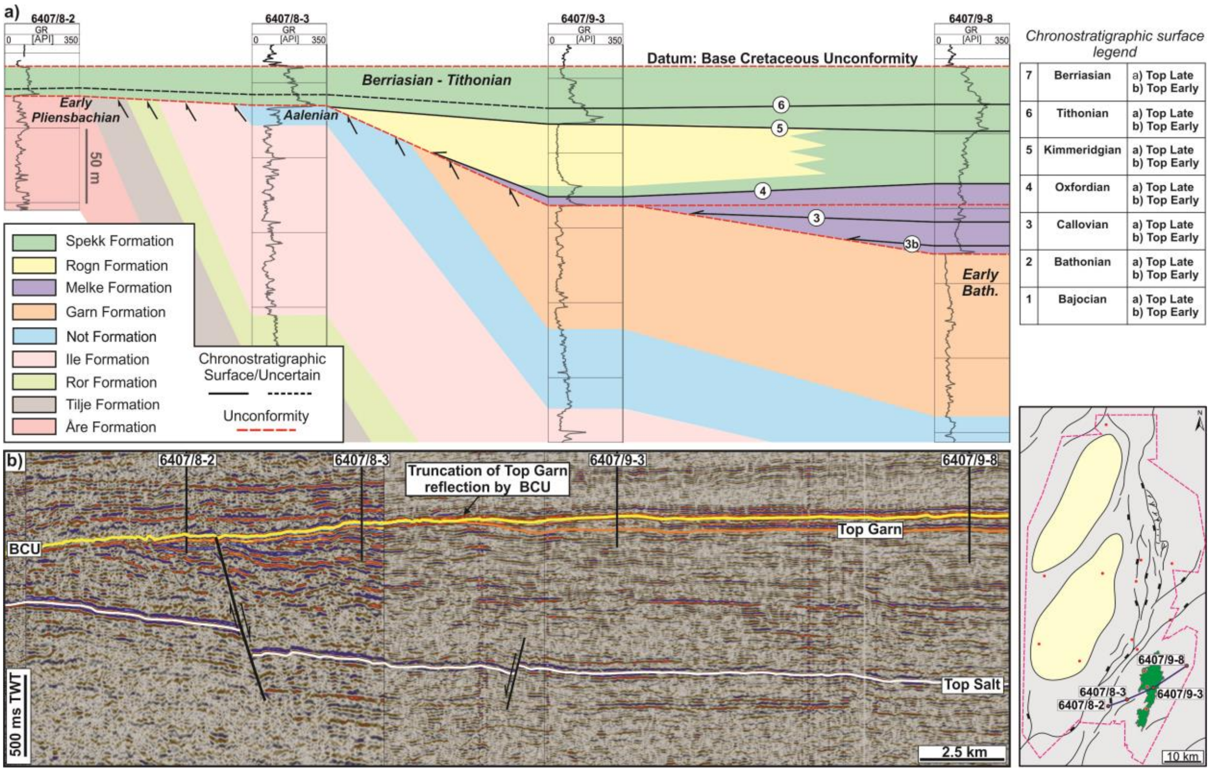

Figure 10: a) Stratigraphic correlation of Jurassic succession from selected wells along a broadly NE-SW along the footwall of the VFC showing the progressive downcutting of the Callovian/Oxfordian composite unconformity to the south where older units subcrop at that erosion level. b) Arbitrary seismic profile used to constrain the underlying structure along the panel in a).

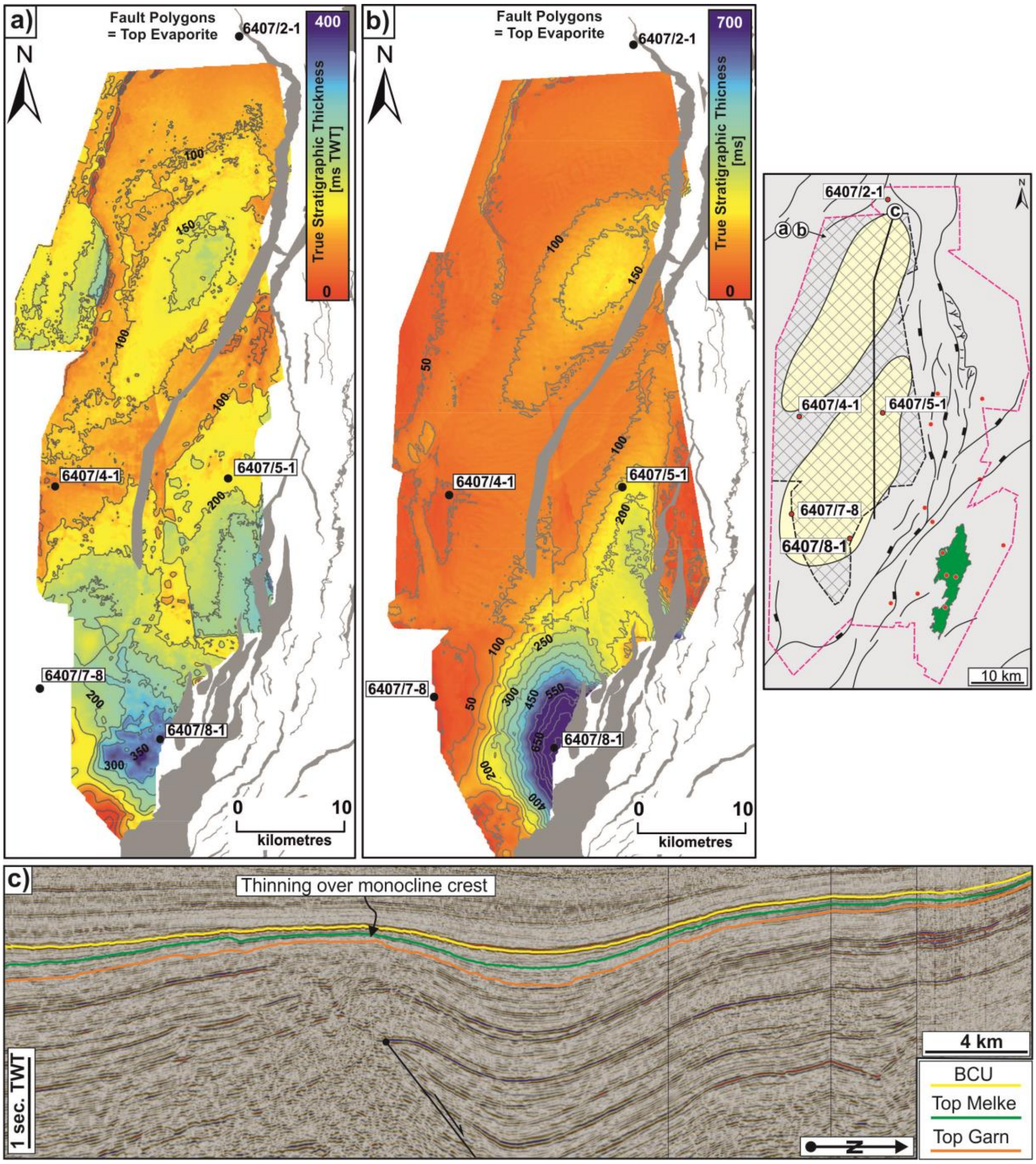

Figure 11: a) Gimsan Basin Melke Formation isochron with Top Evaporite fault polygon and key wells highlighted. Three distinct depocentres are recognised with sediment thicknesses up to 400 ms TWT located within the hangingwall of major faults. b) Spekk Formation isochron from Gimsan Basin with Top Evaporite fault polygons and key wells highlighted. Sediment thicknesses are up to 700 ms TWT found in the immediate SW corner of the basin adjacent to the VFC. c) Seismic profile along the basin axis shows the control that a NE-SW striking structure at depth has upon the Middle to Late Jurassic succession.

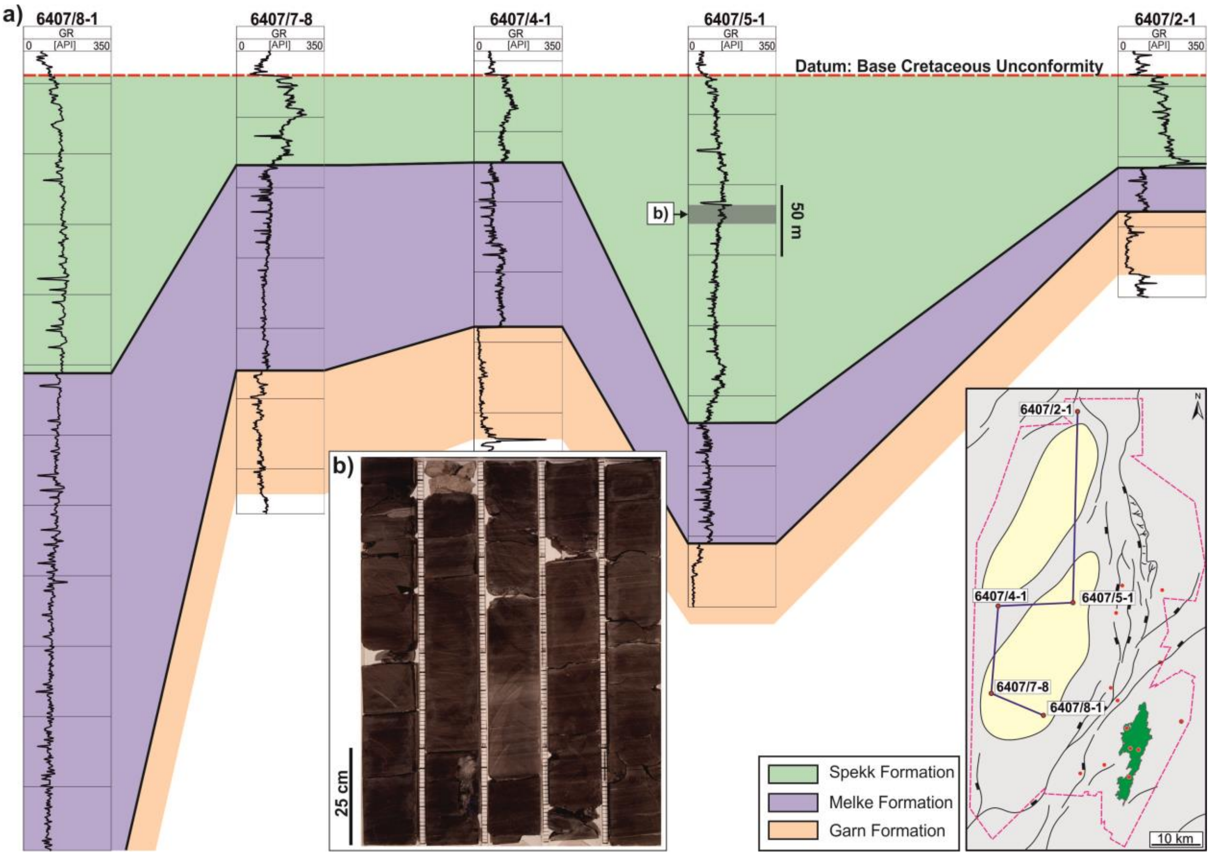

Figure 12: a) Broadly N-S orientated axial lithostratigraphic correlation panel from the Gimsan Basin showing the variations in the Melke and Spekk Formations within the basin. The thickest Melke Formation is found in the SW corner in 6407/8-1 (in the hangingwall of the NE-SW trending VFC) while the thickest Spekk Formation is found further north in 6407/5-1 and comprises shale succession. b) Core photograph from 6407/5-1 within the Spekk Formation showing a predominantly mudstone succession.

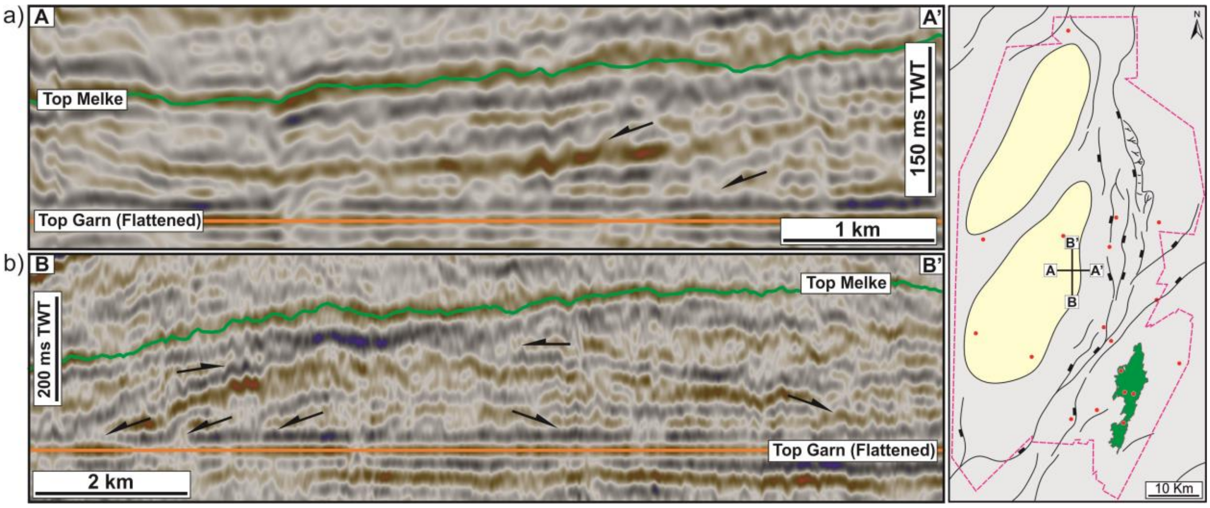

Figure 13: a) E-W orientated seismic profile from the Gimsan Basin, flattened on Top Garn Formation to highlight the downlapping nature of the Melke Formation which thickens towards the VFC. b) N-S seismic profile taken broadly parallel to the VFC, again flattened on Top Garn, showing the mounded nature of the Melke Formation in this area. The onlaps onto the mound flanks suggest positive topography at time of deposition and these interpreted as submarine fan systems of likely Mid to Late Oxfordian age (i.e. intra Melke sandstones comparable to those drilled in the Fenja area to the SW).

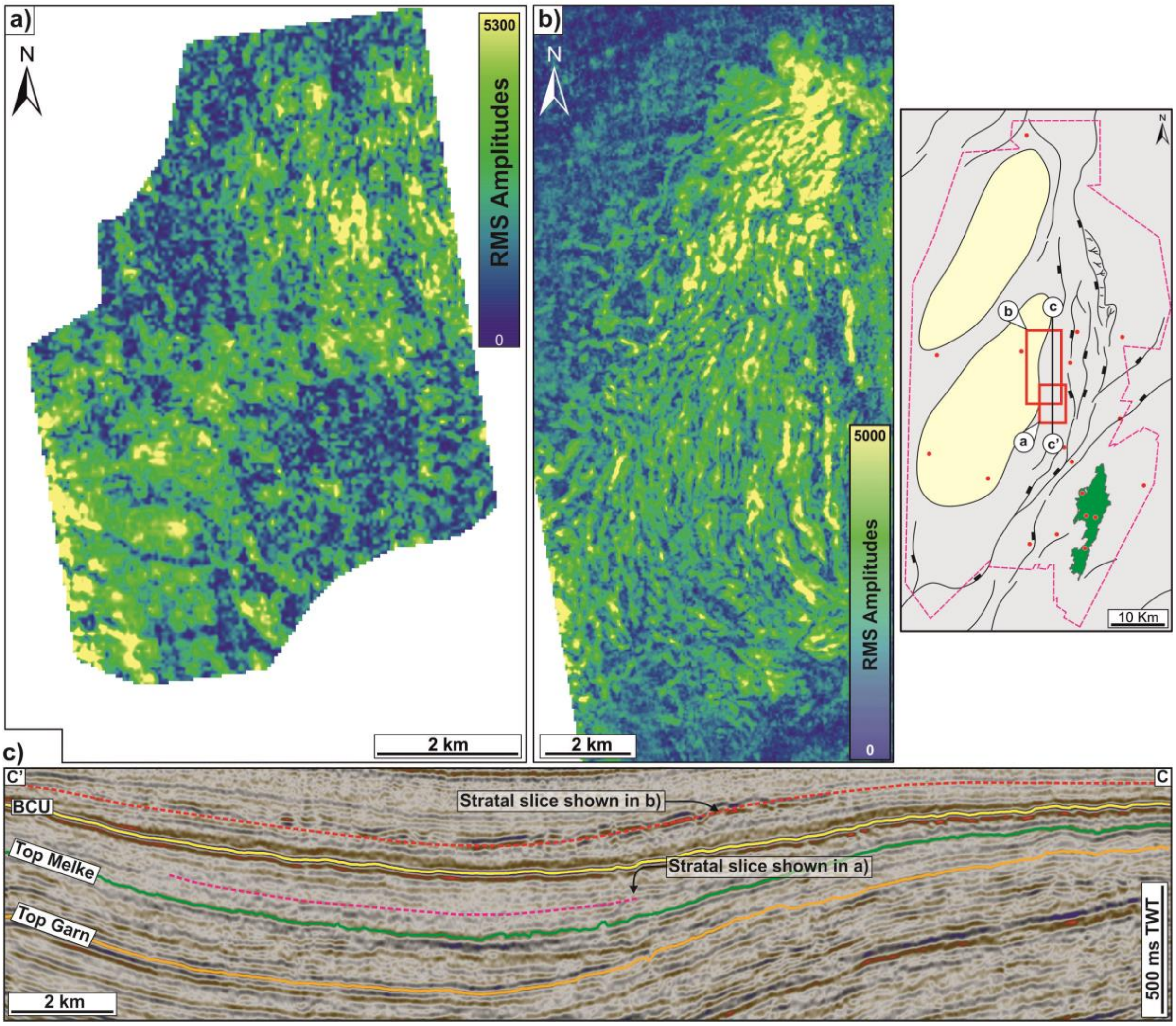

Figure 14: a) RMS amplitude extraction from intra-Spekk reflection event showing high amplitude curvi-linear anomalies expanding away from the Vingleia Fault Complex in the east. b) RMS extraction from Early Cretaceous reflection event described by Løseth et al., (2011) as a large slope failure complex comprised of Spekk Formation shale which exhibits a similar curvi-linear pattern as seen in the intra-Spekk event suggesting a slope failure origin for those features. c) Seismic profile orientated N-S showing the deformation at intra-Spekk Formation level and also in the Early Cretaceous section as described by Løseth et al. (2011).

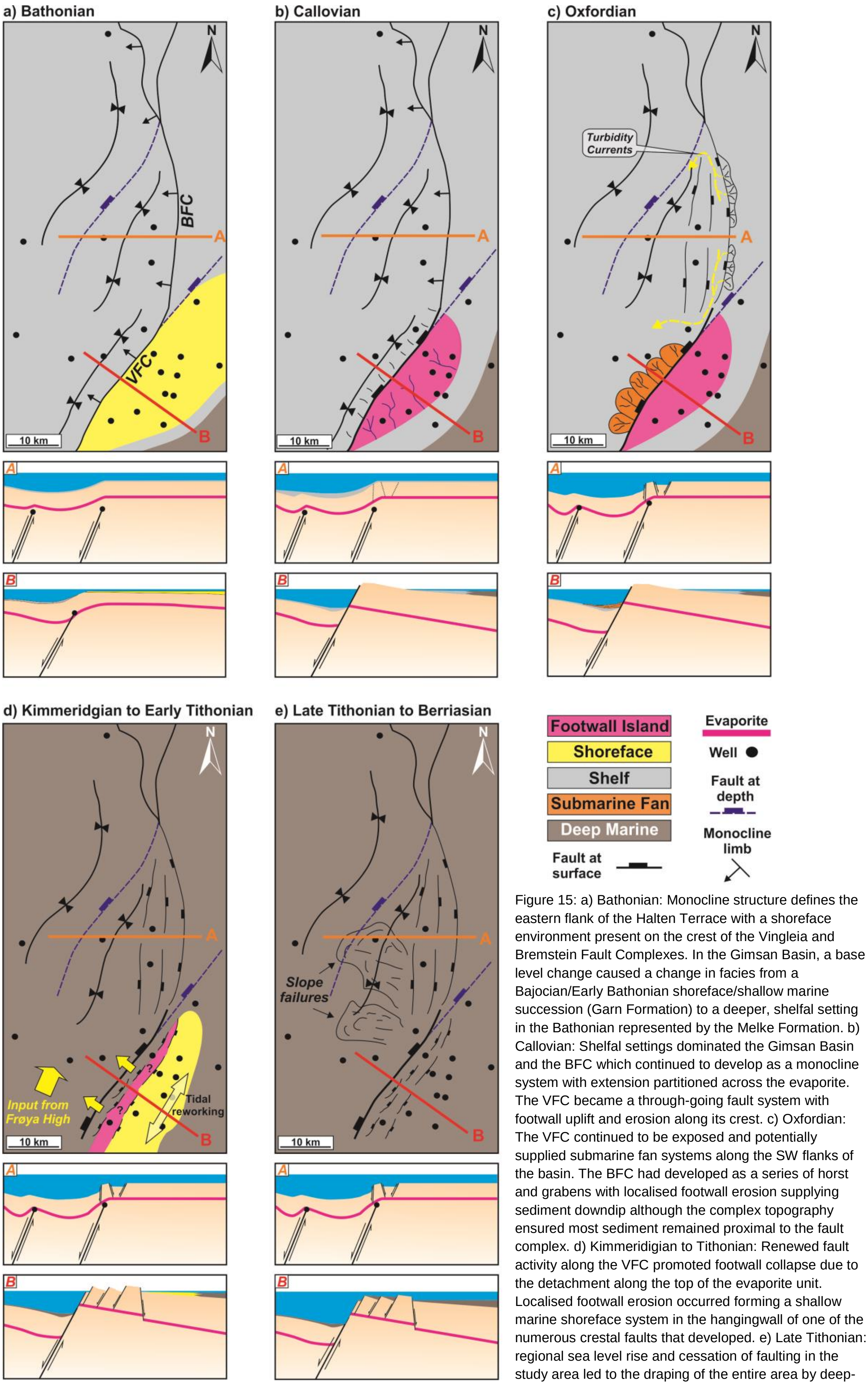

1219 Figure 15: a) Bathonian: Monocline structure defines the eastern flank of the Halten Terrace with a shoreface environment present on the crest of the Vingleia and Bremstein Fault Complexes. In the Gimsan Basin, a base level change caused a change in facies from a Bajocian/Early Bathonian shoreface/shallow marine succession (Garn Formation) to a deeper, shelfal setting in the Bathonian represented by the Melke Formation. b) Callovian: Shelfal settings dominated the Gimsan Basin and the BFC which continued to develop as a monocline system with extension partitioned across the evaporite. The VFC became a through-going fault system with footwall uplift and erosion along its crest. c) Oxfordian: The VFC continued to be exposed and potentially supplied submarine fan systems along the SW flanks of the basin. The BFC had developed as a series of horst and grabens with localised footwall erosion supplying sediment downdip although the complex topography ensured most sediment remained proximal to the fault complex. d) Kimmeridgian to Tithonian: Renewed fault activity along the VFC promoted footwall collapse due to the detachment along the top of the evaporite unit. Localised footwall erosion occurred forming a shallow marine shoreface system in the hangingwall of one of the numerous crestal faults that developed. e) Late Tithonian: regional sea level rise and cessation of faulting in the study area led to the draping of the entire area by deep-marine shales of the Spekk Formation.

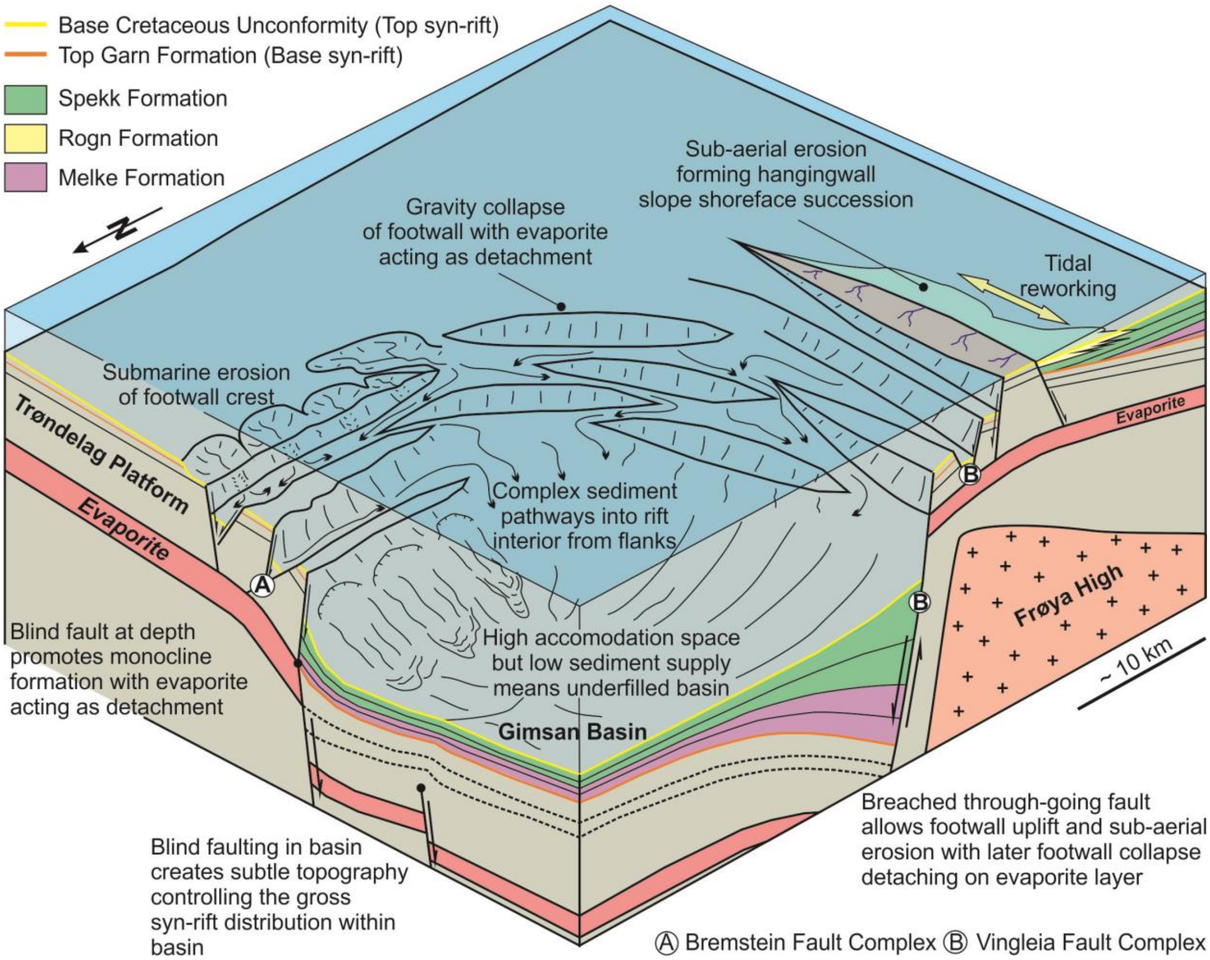

Figure 16: Summary block diagram showing the influence an evaporite sequence can have upon the development of rift flank sedimentary systems. The variable topography along the rift flanks will promote local sediment supply along with small, localised accommodation space which means that syn-rift sediment accumulation will be localised along the rift flank with limited supply deeper into the rift basin.

Well	*Structural Location*	*Melke Fm Thickness (m)*	*Rogn Fm Thickness (m)*	*Spekk Fm Thickness (m)*
6407/2-1	Gimsan Basin	31	0	66
6407/4-1	Gimsan Basin	117	0	62
6407/5-1	Gimsan Basin	86	0	247
6407/6-1	Trondelag Platform	13	0	8
6407/6-4	BFC	73	0	42
6407/6-7S	BFC	0	44	77
6407/7-8	Gimsan Basin	145	0	67
6407/8-1	Gimsan Basin	344	0	212
6407/8-2	VFC Footwall	0	0	0
6407/8-3	VFC Footwall	0	0	27
6407/8-4 S	VFC Footwall	0	0	0
6407/9-3	VFC Footwall	0	38	54
6407/9-4	VFC Footwall	0	2	21
6407/9-5	VFC Footwall	0	51	62
6407/9-6	VFC Footwall	0	17	32
6407/9-8	VFC Footwall	31	0	94
6407/9-9	VFC Footwall	0	0	9

Table 1: Summary table of wells used in the present study with Middle to Late Jurassic thicknesses shown (taken from Norwegian Petroleum Directorate database April 2012).